Casimir densities from coexisting vacua

S. Bellucci,[1,*] A. A. Saharian,[2,†] and A. H. Yeranyan[3,1,2,‡]

[1]*INFN, Laboratori Nazionali di Frascati, Via Enrico Fermi 40, 00044 Frascati, Italy*
[2]*Department of Physics, Yerevan State University, 1 Alex Manoogian Street, 0025 Yerevan, Armenia*
[3]*Museo Storico della Fisica e Centro Studi e Ricerche Enrico Fermi,*
Via Panisperna 89A, 00184 Roma, Italy

The Wightman function, the vacuum expectation values (VEVs) of the field squared, and the energy-momentum tensor are investigated for a massive scalar field with general curvature coupling in a spherically symmetric static background geometry described by two distinct metric tensors inside and outside a spherical boundary. The exterior and interior geometries can correspond to different vacuum states of the same theory. In the region outside the sphere, the contributions in the VEVs, induced by the interior geometry, are explicitly separated. For the special case of the Minkowskian exterior geometry, the asymptotics of the VEVs near the boundary and at large distances are discussed in detail. In particular, it has been shown that the divergences on the boundary are weaker than in the problem of a spherical boundary in Minkowski spacetime with Dirichlet or Neumann boundary conditions. As an application of general results, de Sitter (dS) and anti–de Sitter (AdS) spaces are considered as examples of the interior geometry. For AdS interiors there are no bound states. In the case of dS geometry and for nonminimally coupled fields, bound states appear for a radius of the separating boundary sufficiently close to the dS horizon. Starting from a critical value of the radius, the Minkowskian vacuum in the exterior region becomes unstable. For small values of the AdS curvature radius, to the leading order, the VEVs in the exterior region coincide with those for a spherical boundary in Minkowski spacetime with a Dirichlet boundary condition. The exceptions are the cases of minimal and conformal couplings: for a minimal coupling, the VEVs are reduced to the case with a Neumann boundary condition, whereas for a conformally coupled field there is no reduction to Dirichlet or Neumann results.

I. INTRODUCTION

In many physical problems, the model is formulated in backgrounds having boundaries on which the dynamical variables obey prescribed boundary conditions. The boundaries can have different physical origins, like interfaces between two media with different electromagnetic properties in condensed matter physics, horizons in gravitational physics, domain walls of various physical natures in the theory of phase transitions and critical phenomena, and branes in string theory and in higher-dimensional cosmologies. In quantum field theory, the imposition of boundary conditions on a field operator gives rise to modifications of the spectrum for the vacuum fluctuations of a quantum field and, as a result, to the change of physical characteristics of the vacuum state, such as the energy density and vacuum stresses. As a consequence of this, vacuum forces arise, acting on constraining boundaries. This is the familiar Casimir effect, first predicted for the electromagnetic field by Casimir in 1948 [1]. This effect can have important implications on all scales, from subnuclear to cosmological,

and it has been investigated for various types of bulk and boundary geometries (for reviews see [2]–[6]). The features of the Casimir forces depend on the nature of a quantum field, on the type of the spacetime manifold, on the geometry of boundaries, and on the specific boundary conditions imposed on the field. The explicit dependence can be found for highly symmetric geometries only.

In consideration of the Casimir effect, usually, the boundaries separate the regions with different electromagnetic properties (for example, media with different dielectric permittivities). Another type of effect related to the Casimir physics arises in a class of models with boundaries separating the spatial regions with different gravitational backgrounds. It can be referred to as gravitationally induced Casimir effect. The different gravitational backgrounds on both sides of the separating boundary can correspond to different vacuum states of the same theory. For example, one can consider a bubble of a false vacuum embedded in a true vacuum or vice versa. Simple examples of vacuum bubbles are de Sitter (dS) and anti–de Sitter (AdS) spacetimes embedded in the Minkowski spacetime. In these examples, a physical boundary separates two regions with different values of the cosmological constant. It serves as a thin-wall approximation of a domain wall interpolating between two coexisting vacua (for a discussion, see [7]).

*[*]bellucci@lnf.infn.it
[†]saharian@ysu.am
[‡]ayeran@lnf.infn.it

In a configuration with coexisting gravitational backgrounds, the geometry of one region affects the properties of the quantum vacuum in the other region. Previously, we have considered several examples of this type of vacuum polarization. In [8], the Casimir densities are investigated for a scalar field in the geometry of a cosmic string for a core with finite support. In the corresponding model, the cylindrical boundary separates two different background geometries: the spacetime outside the boundary is described by the idealized cosmic string geometry with a planar angle deficit and for the interior geometry a general cylindrically symmetric static model is employed. Two specific models of the core have been considered: the "ballpoint pen" model [9,10], with a constant curvature interior metric, and the "flower pot" model [11] with an interior Minkowskian spacetime. Similar problems for the exterior geometry of a global monopole are discussed in [12] and [13] for scalar and fermionic fields, respectively. In the corresponding models the boundary separating different spatial geometries is a sphere. The model with a sphere as a boundary and with an exterior dS metric, described in planar inflationary coordinates, has been considered in [14]. The vacuum expectation values (VEVs) of the field squared and the energy-momentum tensor induced by a Z_2-symmetric brane with finite thickness located on the AdS background are evaluated in [15,16] for a massive scalar field. The general case of a static plane symmetric interior structure for the brane is considered, and the exterior AdS geometry is described in Poincaré coordinates. In the corresponding problem the separating boundaries are plane symmetric.

In the present paper, we consider the vacuum densities for a massive scalar field with a general curvature coupling parameter in a spherically symmetric static geometry described by two distinct metric tensors inside and outside a spherical boundary. In addition, the presence of a surface energy-momentum tensor located on the separating boundary is assumed. Among the most important characteristics of the quantum vacuum are the expectation values of the field squared and the energy-momentum tensor. Although the corresponding operators are local, due to the global nature of the vacuum state, they carry important information about the global properties of the bulk. Moreover, in addition to describing the physical structure of the quantum field at a given point, the VEV of the energy-momentum tensor acts as a source of gravity in the quasiclassical Einstein equations. Consequently, it plays a crucial role in modeling a self-consistent dynamic of the background spacetime. For the evaluation of the VEVs, we first construct the positive frequency Wightman function by the direct summation over a complete set of scalar modes. This function also determines the excitation probability of a Unruh-DeWitt detector (see, for instance, [17]). The quantum effects induced by distinct geometries in the exterior and interior regions should be taken into account,

in particular, in discussions of the dynamics of vacuum bubbles during the phase transitions in the early Universe.

The organization of the paper is as follows. In the next section we describe the background spacetime under consideration and the matching conditions on a spherical boundary separating the interior and exterior geometries. A complete set of normalized mode functions for a scalar field with a general curvature coupling parameter is constructed in Sec. III. By using the mode functions, in Sec. IV we evaluate the positive frequency Wightman function for the general case of static spherically symmetric interior and exterior geometries. This function is presented in the form where the contribution induced by the interior geometry is explicitly separated. A special case of the exterior Minkowskian background is considered in Sec. V. Explicit expressions for the VEVs of the field squared and of the energy-momentum tensor are provided and their behavior in asymptotic regions of the parameters is investigated. As an application of general results, in Sec. VI, two special cases of the interior geometry are discussed corresponding to maximally symmetric spaces with positive and negative cosmological constants (dS and AdS spaces). Section VII summarizes the main results of the paper. In Appendix A, the coefficient in the asymptotic expansion of the logarithmic derivative of the hypergeometric function is determined, which is used for the evaluation of the leading terms in the asymptotic expansions of the VEVs near the boundary for the cases of the interior dS and AdS spaces.

II. BACKGROUND GEOMETRY

Consider a $(D + 1)$-dimensional spherically symmetric static spacetime described by two distinct metric tensors inside and outside of a spherical boundary of the coordinate radius $r = a$. In the interior region, $r < a$, the spacetime geometry is regular with the line element

$$ds_i^2 = e^{2u_i(r)}dt^2 - e^{2v_i(r)}dr^2 - e^{2w_i(r)}d\Omega_{D-1}^2, \quad (2.1)$$

where $d\Omega_{D-1}^2$ is the line element on a $(D-1)$-dimensional sphere with a unit radius. The corresponding hyperspherical angular coordinates will be denoted by $(\vartheta, \phi) = (\theta_1, \ldots, \theta_n, \phi)$, where $n = D - 2$, $0 \leq \theta_k \leq \pi$, $k = 1, \ldots, n$, and $0 \leq \phi \leq 2\pi$. The value of the radial coordinate r corresponding to the center of the configuration will be denoted by r_c. Of course, we could rescale the radial coordinate in order to have $r = 0$ for the center, but for the further discussion it is convenient to keep r_c general. Introducing a new coordinate,

$$\bar{r} = e^{w_i(r)}, \quad (2.2)$$

with the center at $\bar{r} = 0$, the angular components of the metric tensor coincide with the corresponding components

in the Minkowski spacetime described in the standard hyperspherical coordinates.

In the exterior region, $r > a$, the geometry has a similar structure with different radial functions:

$$ds_e^2 = e^{2u_e(r)}dt^2 - e^{2v_e(r)}dr^2 - e^{2w_e(r)}d\Omega_{D-1}^2. \quad (2.3)$$

The metric tensor is continuous at the separating boundary $r = a$:

$$u_i(a) = u_e(a), \quad v_i(a) = v_e(a), \quad w_i(a) = w_e(a). \quad (2.4)$$

Although the scheme described below can be generalized for metric tensors with horizons, for the sake of simplicity we will assume that if the line elements (2.1) and (2.3) have horizons at r_{Hi} and r_{He}, respectively, then $r_{He} < a < r_{Hi}$. This means that the combined geometry contains no horizons.

The Ricci tensors for the interior and exterior geometries are diagonal with the mixed components (no summation over $l = 2, 3, ..., D$):

$$R^0_{(j)0} = -e^{-2v_j}[u_j'' + u_j'^2 - u_j'v_j' + (n+1)u_j'w_j'],$$

$$R^1_{(j)1} = -e^{-2v_j}[u_j'' + u_j'^2 - u_j'v_j' + (n+1)(w_j'' + w_j'^2 - w_j'v_j')],$$

$$R^l_{(j)l} = -e^{-2v_j}(w_j'' + w_j'^2 + w_j'u_j' - w_j'v_j' + nw_j'^2) + ne^{-2w_j}, \quad (2.5)$$

where $j = i$ and $j = e$ for the interior and exterior regions, respectively, and the prime means the derivative with respect to the radial coordinate r (we adopt the convention of Ref. [17] for the curvature tensor). For the corresponding Ricci scalars, we get the expression

$$R_{(j)} = -2e^{-2v_j}[u_j'' + u_j'^2 - u_j'v_j' + n(n+1)w_j'^2/2$$
$$+(n+1)(w_j'' + w_j'^2 + w_j'u_j' - w_j'v_j')]$$
$$+ n(n+1)e^{-2w_j}. \quad (2.6)$$

The energy-momentum tensors generating the line elements (2.1) and (2.3) are found from the corresponding Einstein equations.

In general, we assume the presence of an infinitely thin spherical shell at $r = a$, having a surface energy-momentum tensor τ_i^k with nonzero components τ_0^0 and $\tau_2^2 = \cdots = \tau_D^D$. Let n^i, $n_i n^i = -1$, be the normal to the shell that points into the bulk on both sides. For the interior $(j = i)$ and exterior $(j = e)$ regions, one has $n_i^{(j)} = \delta_{(j)}\delta_i^l e^{v_j(r)}$ with $\delta_{(i)} = 1$ and $\delta_{(e)} = -1$. We denote by $h_{(j)ik}$ the induced metric on the shell, $h_{(j)ik} = g_{(j)ik} + n_i^{(j)}n_k^{(j)}$, and $K_{(j)ik} = h_{(j)i}^l h_{(j)k}^r \nabla_l n_r^{(j)}$ is the extrinsic curvature of the latter, we obtain

$$K^0_{(j)0} = -\delta_{(j)}u_j'(r)e^{-v_j(r)},$$

$$K^k_{(j)l} = -\delta_{(j)}\delta_l^k w_j'(r)e^{-v_j(r)}, \quad r = a - \delta_{(j)}0, \quad (2.7)$$

with $l = 2, 3, ..., D$.

From the Israel matching conditions on the sphere $r = a$, one has

$$\sum_{j=i,e}(K_{(j)ik} - K_{(j)}h_{(j)ik}) = 8\pi G\tau_{ik}, \quad (2.8)$$

where G is the gravitational constant and $K_{(j)} = K^i_{(j)i}$ is the trace of the extrinsic curvature tensor. From these conditions, by taking into account (2.7), we find (with no summation over $i = 2, 3, ..., D$)

$$\sum_{j=i,e}\delta_{(j)}u_j'(a - \delta_{(j)}0) = 8\pi Ge^{v_e(a)}\left(\tau_i^i - \frac{D-2}{D-1}\tau_0^0\right),$$

$$\sum_{j=i,e}\delta_{(j)}w_j'(a - \delta_{(j)}0) = \frac{8\pi G}{D-1}e^{v_e(a)}\tau_0^0, \quad (2.9)$$

where $f'(a \pm 0)$ is understood as the limit $\lim_{r \to a\pm 0}f'(r)$. Note that from (2.9) the relation

$$\sum_{j=i,e}\delta_{(j)}[u_j'(a - \delta_{(j)}0) + (D-1)w_j'(a - \delta_{(j)}0)] = \frac{8\pi G}{D-1}e^{v_e(a)}\tau \quad (2.10)$$

is obtained for the trace $\tau = \tau_0^0 + \sum_{i=2}^D \tau_i^i$ of the surface energy-momentum tensor. For given interior and exterior geometries, the relations (2.9) determine the surface energy-momentum tensor needed for the matching of these geometries.

III. MODE FUNCTIONS FOR A SCALAR FIELD

A. Modes of continuous spectrum

Having described the background geometry, now we turn to the field content. We will consider a scalar field $\varphi(x)$ with the curvature coupling parameter ξ on the background described by (2.1) and (2.3). The corresponding field equation reads

$$(\nabla_\mu\nabla^\mu + m^2 + \xi R)\varphi = 0, \quad (3.1)$$

where ∇_μ is the covariant derivative operator. The most important special cases of the curvature coupling parameter $\xi = 0$ and $\xi = \xi_D = (D-1)/(4D)$ correspond to minimally and to conformally coupled fields, respectively.

In addition to the field equation in the regions $r < a$ and $r > a$, the matching conditions for the field should be specified at $r = a$. The field is continuous on the separating surface: $\varphi|_{r=a-0} = \varphi|_{r=a+0}$. In order to find the matching

condition for the radial derivative of the field, we note that the discontinuity of the functions $u'(r)$ and $w'(r)$ at $r = a$ leads to the delta function term

$$2e^{-2v_e(a)}\sum_{j=i,e}\delta_{(j)}[u'_j(a-\delta_{(j)}0)+(D-1)w'_j(a-\delta_{(j)}0)]\delta(r-a)$$

$$(3.2)$$

in the Ricci scalar and, hence, in the field equation (3.1), if we require its validity everywhere in the space. The expression (3.2) is given in terms of the trace of the surface energy-momentum tensor by using the formula (2.10). As a result of the presence of the delta function term in the field equation, the radial derivative of the field has a discontinuity at $r = a$. The jump condition is obtained by integrating the field equation through the point $r = a$. This gives

$$(\partial_r\varphi)_{r=a+0} - (\partial_r\varphi)_{r=a-0} = \frac{16\pi G\xi}{D-1}e^{v_e(a)}\tau\varphi|_{r=a}. \quad (3.3)$$

For a minimally coupled field, the radial derivative is continuous.

In what follows, we are interested in the VEVs of the field squared and of the energy-momentum tensor induced in the region $r > a$ by the geometry in $r < a$. In the model under consideration all the information about the properties of the vacuum is encoded in two-point functions. As such, we will use the positive frequency Wightman function defined as the VEV $W(x, x') = \langle 0|\varphi(x)\varphi(x')|0\rangle$, where $|0\rangle$ stands for the vacuum state. In addition to describing the local properties of the vacuum, this function also determines the response of the Unruh-DeWitt type particle detectors [17]. For the evaluation of the Wightman function, we will use the direct summation over a complete set of positive- and negative-energy mode functions $\{\varphi_\alpha(x), \varphi_\alpha^*(x')\}$, obeying the field equation (3.1) and the matching conditions described above. Here, the set of quantum numbers α specifies the solutions. Expanding the field operator over the complete set $\{\varphi_\alpha(x), \varphi_\alpha^*(x')\}$ and using the standard commutation relations for the annihilation and creation operators, the following mode-sum formula is readily obtained:

$$W(x, x') = \sum_\alpha \varphi_\alpha(x)\varphi_\alpha^*(x'), \quad (3.4)$$

where we assume summation over discrete quantum numbers and integration over continuous ones.

In the problem under consideration, the mode functions can be presented in the factorized form

$$\varphi_\alpha(x) = f_l(r)Y(m_k; \vartheta, \phi)e^{-i\omega t}, \quad (3.5)$$

where $l = 0, 1, 2, \ldots$, $Y(m_k; \vartheta, \phi)$ is the hyperspherical harmonic of the degree l [18], $m_k = (m_0 \equiv l, m_1, \ldots, m_n)$, with $m_1, m_2, \ldots, m_n$ being integers such that

$$0 \le m_{n-1} \le m_{n-2} \le \cdots \le m_1 \le l,$$
$$-m_{n-1} \le m_n \le m_{n-1}. \quad (3.6)$$

Presenting the radial function as

$$f_l(r) = \begin{cases} f_{(i)l}(r), & r < a, \\ f_{(e)l}(r) & r > a, \end{cases} \quad (3.7)$$

the equations for the exterior and interior functions are obtained from (3.1):

$$f''_{(j)l}(r) + [u'_j - v'_j + (D-1)w'_j]f'_{(j)l}(r)$$
$$+ e^{2v_j}\left[\frac{\omega^2}{e^{2u_j}} - m^2 - \xi R_{(j)} - \frac{l(l+n)}{e^{2w_j}}\right]f_{(j)l}(r) = 0, \quad (3.8)$$

where the Ricci scalar is given by the expression (2.6). From the matching conditions on the separating boundary, given above, for the radial functions in the interior and exterior regions, we find $f_{(e)l}(a + 0) = f_{(i)l}(a - 0)$ and

$$f'_{(e)l}(a + 0) - f'_{(i)l}(a - 0) = \frac{16\pi G\xi}{D-1}e^{v_e(a)}\tau f_{(e)l}(a). \quad (3.9)$$

Note that, introducing a new radial coordinate, Eq. (3.8) can be written in the Schrödinger-like form

$$\partial_y^2 g_{(j)l}(y) + [\omega^2 - U_{(j)l}(y)]g_{(j)l}(y) = 0, \quad (3.10)$$

where

$$g_{(j)l}(y) = e^{(D-1)w_j/2}f_{(j)l}(r), \quad y = \int dr e^{v_j - u_j}, \quad (3.11)$$

and for the potential function we have

$$U_{(j)l}(y) = e^{2u_j}\left[m^2 + \xi R_{(j)} + \frac{l(l+n)}{e^{2w_j}}\right]$$
$$+ \frac{D-1}{2}\left(w''_j + \frac{D-1}{2}w'^2_j\right). \quad (3.12)$$

In what follows we assume that the interior geometry is regular. In terms of the radial coordinate (2.2), from the regularity of the Ricci scalar (2.6) at the center, $\bar{r} = 0$, it follows that

$$u_i(\bar{r}), \quad v_i(\bar{r}) \sim \bar{r}^2, \quad \bar{r} \to 0. \quad (3.13)$$

Let $f^{(1)}_{(i)l}(r, \lambda)$, with $\lambda^2 = \omega^2 - m^2$, be the solution of Eq. (3.8) in the interior region that is regular at the origin. It can be taken as a real function. In addition, by taking into account that λ enters in the equation in the form λ^2, without loss of generality we can assume that $f^{(1)}_{(i)l}(r, -\lambda) = $ const $\cdot f^{(1)}_{(i)l}(r, \lambda)$. From the regularity of the geometry at

the center and from (3.8), it follows that near the center the interior regular solution behaves as $f_{(i)l}^{(1)}(r,\lambda) \sim \bar{r}^l$.

Now the radial parts of the mode functions are presented as

$$f_l(r) = \begin{cases} A_{(i)}f_{(i)l}^{(1)}(r,\lambda), & \text{for } r < a \\ A_{(e)1}f_{(e)l}^{(1)}(r,\lambda) + A_{(e)2}f_{(e)l}^{(2)}(r,\lambda), & \text{for } r > a \end{cases},$$
$$(3.14)$$

where $f_{(e)l}^{(1)}(r,\lambda)$ and $f_{(e)l}^{(2)}(r,\lambda)$ are the two linearly independent solutions of the radial equation in the exterior region [Eq. (3.8) with $j = e$]. We assume that the functions $f_{(e)l}^{(j)}(r,\lambda)$, $j = 1,2$, are taken to be real. The coefficients in (3.14) are determined by the continuity condition for the radial functions and by the jump condition (3.9) for their radial derivatives. From these conditions, we get

$$A_{(e)1} = A_{(i)}W_l^{(1)}, \qquad A_{(e)2} = -A_{(i)}W_l^{(2)}, \quad (3.15)$$

with the notations

$$W_l^{(1)} = \frac{W_l^{(i2)}(a,\lambda)}{W_l^{(12)}(a)} - \frac{16\pi G\xi}{D-1}e^{v_e(a)}\tau\frac{f_{(i)l}^{(1)}(a,\lambda)}{W_l^{(12)}(a)}f_{(e)l}^{(2)}(a,\lambda),$$

$$W_l^{(2)} = \frac{W_l^{(i1)}(a,\lambda)}{W_l^{(12)}(a)} - \frac{16\pi G\xi}{D-1}e^{v_e(a)}\tau\frac{f_{(i)l}^{(1)}(a,\lambda)}{W_l^{(12)}(a)}f_{(e)l}^{(1)}(a,\lambda).$$
$$(3.16)$$

In (3.16) we have defined the functions

$$W_l^{(ij)}(r,\lambda) = W\{f_{(i)l}^{(1)}(r,\lambda), f_{(e)l}^{(j)}(r,\lambda)\}, \quad j = 1,2$$

$$W_l^{(12)}(r) = W\{f_{(e)l}^{(1)}(r,\lambda), f_{(e)l}^{(2)}(r,\lambda)\}, \quad (3.17)$$

where $W\{f(r), g(r)\} = f(r)g'(r) - f'(r)g(r)$ is the Wronskian. The Wronskian $W_l^{(12)}(r)$ can be found from Eq. (3.8) with $j = e$:

$$W_l^{(12)}(r) = Ce^{-u_e(r)+v_e(r)-(D-1)w_e(r)}, \quad (3.18)$$

where the constant C is determined by the choice of the functions $f_{(e)l}^{(1)}(r,\lambda)$ and $f_{(e)l}^{(2)}(r,\lambda)$. Here, we will assume that the exterior metric is asymptotically flat at large distances from the boundary, $r \to \infty$. With this assumption, we can see that for large r the solution for the exterior equation is given by $r^{-n}Z_{\nu_l}(\lambda r)$, where $Z_{\nu_l}(\lambda r)$ is a cylinder function of the order

$$\nu_l = l + n/2. \quad (3.19)$$

If we take the functions $f_{(e)l}^{(1)}(r,\lambda)$ and $f_{(e)l}^{(2)}(r,\lambda)$ such that $f_{(e)l}^{(1)}(r,\lambda) \approx r^{-n/2}J_{\nu_l}(\lambda r)$, $f_{(e)l}^{(2)}(r,\omega) \approx r^{-n/2}Y_{\nu_l}(\lambda r)$, for $r \to \infty$, with $J_\nu(x)$ and $Y_\nu(x)$ being the Bessel and the Neumann functions, then for the constant in (3.18) we find $C = 2/\pi$. In what follows we will assume this choice of the normalization for the exterior mode functions. In this way, as a complete set of quantum numbers specifying the mode functions, we can take the set $\alpha = (\lambda, m_k)$. Here, we assume that λ is real. In addition, bound states can be present with a purely imaginary λ. These states are discussed below.

The remaining coefficient $A_{(i)}$ is determined by the normalization condition for the mode functions given by

$$\int d^D x\sqrt{|g|}g^{00}\varphi_\alpha(x)\overset{\leftrightarrow}{\partial}_t\varphi_{\alpha'}^*(x) = i\delta(\lambda - \lambda')\delta_{m_k m_k'}. \quad (3.20)$$

The integral over $r \leq a$ is finite and the divergence for $\lambda = \lambda'$ comes from the upper limit of the integration over r. As a consequence of this, we can replace the functions $f_{(e)l}^{(1)}(r,\omega)$ and $f_{(e)l}^{(2)}(r,\omega)$ by their asymptotics for $r \to \infty$. In this way, for the normalization coefficient one finds

$$A_{(i)}^2 = \lambda\frac{(W_l^{(1)2} + W_l^{(2)2})^{-1}}{2N(m_k)\omega}, \quad (3.21)$$

with $W_l^{(1,2)}$ given by (3.16). Hence, for the radial mode functions, we get

$$f_l(r,\lambda) = A_{(i)}\begin{cases} f_{(i)l}^{(1)}(r,\lambda), & \text{for } r < a \\ f_{(e)l}(r,\lambda), & \text{for } r > a \end{cases}, \quad (3.22)$$

where the notation

$$f_{(e)l}(r,\lambda) = W_l^{(1)}f_{(e)l}^{(1)}(r,\lambda) - W_l^{(2)}f_{(e)l}^{(2)}(r,\lambda), \quad (3.23)$$

is introduced.

An equivalent form of the exterior mode functions is given by

$$f_l(r,\lambda) = A_{(e)}g_l(r,\lambda), \quad r > a, \quad (3.24)$$

with the notation

$$g_l(r,\lambda) = \bar{f}_{(e)l}^{(2)}(a,\lambda)f_{(e)l}^{(1)}(r,\lambda) - \bar{f}_{(e)l}^{(1)}(a,\lambda)f_{(e)l}^{(2)}(r,\lambda), \quad (3.25)$$

and with the normalization coefficient

$$A_{(e)}^2 = \lambda\frac{[\bar{f}_{(e)l}^{(1)2}(a,\lambda) + \bar{f}_{(e)l}^{(2)2}(a,\lambda)]^{-1}}{2N(m_k)\omega}. \quad (3.26)$$

Here, and in what follows, for a given function $F(r, \lambda)$, we use the notation

$$
\bar{F}(r, \lambda) = \partial_r F(r, \lambda)
$$
$$
- \left[\frac{f_{(i)l}^{(1)\prime}(a, \lambda)}{f_{(i)l}^{(1)}(a, \lambda)} + \frac{16\pi G\xi}{D-1} e^{v_e(a)}\tau \right] F(r, \lambda), \quad (3.27)
$$

where $f_{(i)l}^{(1)\prime}(a, \lambda) = \partial_r f_{(i)l}^{(1)}(r, \lambda)|_{r=a-0}$. Note that one has the relation

$$
A_{(e)} = A_{(i)} \frac{f_{(i)l}^{(1)}(a, \lambda)}{W_l^{(12)}(a)} \quad (3.28)
$$

for the coefficients in the exterior and interior regions.

B. Bound states

In the previous subsection we have considered the modes with a real λ. In addition to them, the modes with an imaginary λ can be present that correspond to possible bound states. For these states, the exterior radial mode functions in the region $r \to \infty$ behave as $r^{-n/2}K_{\nu_l}(\eta r)$, where $\eta = |\lambda|$ and $K_\nu(x)$ is the Macdonald function. In order to have a stable vacuum state we will assume that $\eta < m$. For the radial functions corresponding to the bound states, one has

$$
f_{bl}(r, \lambda) = \begin{cases} A_{(ib)} f_{(ib)l}^{(1)}(r, \eta), & \text{for } r < a \\ A_{(eb)} f_{(eb)l}^{(2)}(r, \eta), & \text{for } r > a \end{cases}, \quad (3.29)
$$

where $f_{(eb)l}^{(2)}(r, \eta) \approx r^{-n/2}K_{\nu_l}(\eta r)$ for $r \to \infty$. The continuity of the mode functions at $r = a$ leads to the relation

$$
A_{(ib)} f_{(ib)l}^{(1)}(a, \eta) = A_{(eb)} f_{(eb)l}^{(2)}(a, \eta). \quad (3.30)
$$

From the jump condition for the radial derivative, we see that the allowed values of η for bound states are solutions of the equation

$$
\hat{f}_{(eb)l}^{(2)}(a, \eta) = 0, \quad (3.31)
$$

where for a function $F(r, \eta)$ we define

$$
\hat{F}(r, \eta) = \partial_r F(r, \eta) - \left[\frac{f_{(ib)l}^{(1)\prime}(a, \eta)}{f_{(ib)l}^{(1)}(a, \eta)} + \frac{16\pi G\xi}{D-1} e^{v_e(a)}\tau \right] F(r, \eta).
$$
$$
\quad (3.32)
$$

The possible solutions of Eq. (3.31) will be denoted by $\eta = \eta_s$, $s = 1, 2, \dots$.

The remaining coefficient in the mode functions (3.29) is determined from the normalization condition for the bound states

$$
A_{(eb)}^{-2} = 2\omega N(m_k) \left[\int_a^\infty dr e^{-u_e+v_e+(D-1)w_e} f_{(eb)l}^{(2)2}(r, \eta) \right.
$$
$$
\left. + \frac{f_{(eb)l}^{(2)2}(a, \eta)}{f_{(i)l}^2(a, \eta)} \int_{r_c}^a dr e^{-u_i+v_i+(D-1)w_i} f_{(ib)l}^{(1)2}(r, \eta) \right],
$$
$$
\quad (3.33)
$$

with $\eta = \eta_s$. In order to evaluate the integrals in this formula, we note that for a solution $f_{(j)\omega l}(r)$ to the radial equation (3.8) the following formula can be proved:

$$
\int dr e^{-u_j+v_j+(D-1)w_j} f_{(j)\omega l}(r) f_{(j)\omega_1 l}(r)
$$
$$
= \frac{e^{u_j-v_j+(D-1)w_j}}{\omega_1^2 - \omega^2} [f'_{(j)\omega l}(r) f_{(j)\omega_1 l}(r) - f_{(j)\omega l}(r) f'_{(j)\omega_1 l}(r)].
$$
$$
\quad (3.34)
$$

In particular, in the limit $\omega_1 \to \omega$, from here one can obtain

$$
\int dr e^{-u_j+v_j+(D-1)w_j} f_{(j)\omega l}^2(r)
$$
$$
= \frac{e^{u_j-v_j+(D-1)w_j}}{2\omega} [f'_{(j)\omega l}(r)\partial_\omega f_{(j)\omega l}(r)
$$
$$
- f_{(j)\omega l}(r)\partial_\omega f'_{(j)\omega l}(r)]. \quad (3.35)
$$

Applying to the integrals in Eq. (3.33) the formula (3.35) with $\omega = \sqrt{m^2 - \eta^2}$ and using the continuity of the radial eigenfunctions at $r = a$, for the normalization coefficient one finds

$$
A_{(eb)}^{-2} = N(m_k) e^{u(a)-v(a)+(D-1)w(a)} f_{(eb)l}^{(2)}(a, \eta)\partial_\omega \hat{f}_{(eb)l}^{(2)}(a, \eta). \quad (3.36)
$$

The coefficient $A_{(i)}$ is found from (3.30).

An equivalent expression for the normalization coefficient is obtained by using the Wronskian relation

$$
f_{(eb)l}^{(2)}(a, \eta) f_{(eb)l}^{(1)\prime}(a, \eta) - f_{(eb)l}^{(1)}(a, \eta) f_{(eb)l}^{(2)\prime}(a, \eta)
$$
$$
= e^{-u_e(a)+v_e(a)-(D-1)w_e(a)} \quad (3.37)
$$

for two linearly independent solutions of the radial equation in the exterior region. Here, the function $f_{(eb)l}^{(1)}(r, \eta)$ is normalized by the relation $f_{(eb)l}^{(1)}(r, \eta) \approx r^{-n/2}I_{\nu_l}(\eta r)$ for $r \to \infty$, with $I_\nu(x)$ being the modified Bessel function. From (3.37) we get

$$
f_{(eb)l}^{(2)}(a, \eta) \hat{f}_{(eb)l}^{(1)}(a, \eta) - f_{(eb)l}^{(1)}(a, \eta) \hat{f}_{(eb)l}^{(2)}(a, \eta)
$$
$$
= e^{-u_e(a)+v_e(a)-(D-1)w_e(a)}. \quad (3.38)
$$

By taking into account that for the bound states one has Eq. (3.31), this gives

$$f^{(2)}_{(eb)l}(a, \eta_s) = \frac{e^{-u_e(a)+v_e(a)-(D-1)w_e(a)}}{\hat{f}^{(1)}_{(eb)l}(a, \eta_s)}.$$

Hence, the normalization constant for the exterior modes is written in the form

$$A^2_{(eb)} = -\frac{\eta \hat{f}^{(1)}_{(eb)l}(a, \eta)}{N(m_k) \omega \partial_\eta \hat{f}^{(2)}_{(eb)l}(a, \eta)}, \qquad (3.39)$$

with $\eta = \eta_s$.

IV. WIGHTMAN FUNCTION

Having a complete set of modes, we can proceed to the evaluation of the Wightman function by using the mode sum formula (3.4). First, we consider the case with no bound states. Substituting the functions (3.5) in (3.4), the summation over m_k is done by using the addition formula for the hyperspherical harmonics [18]:

$$\sum_{m_k} \frac{Y(m_k; \vartheta, \phi)}{N(m_k)} Y^*(m_k; \vartheta', \phi') = \frac{2l+n}{nS_D} C^{n/2}_l(\cos\theta), \quad (4.1)$$

where θ is the angle between the directions determined by the angles (ϑ, ϕ) and (ϑ', ϕ'). In (4.1), $S_D = 2\pi^{D/2}/\Gamma(D/2)$ is the surface area of the unit sphere in D-dimensional space and $C^p_l(x)$ is the Gegenbauer polynomial of degree l and order p. With the modes (3.24) and the normalization coefficient (3.26), the expression for the Wightman function in the exterior region reads

$$W(x, x') = \sum_{l=0}^{\infty} \frac{l+n/2}{nS_D} C^{n/2}_l(\cos\theta)$$
$$\times \int_0^\infty d\lambda \frac{\lambda}{\omega} \frac{g_l(r, \lambda)g_l(r', \lambda)e^{-i\omega\Delta t}}{\bar{f}^{(1)2}_{(e)l}(a, \lambda) + \bar{f}^{(2)2}_{(e)l}(a, \lambda)}, \quad (4.2)$$

where $\Delta t = t - t'$ and the function $g_l(r, \lambda)$ is defined by (3.25).

In order to separate from the Wightman function the contribution induced by the interior geometry, first we introduce the functions

$$f^{(\pm)}_{(e)l}(r, \lambda) = f^{(1)}_{(e)l}(r, \lambda) \pm i f^{(2)}_{(e)l}(r, \lambda). \qquad (4.3)$$

Note that, as the functions $f^{(1)}_{(e)l}(r, \lambda)$ and $f^{(2)}_{(e)l}(r, \lambda)$ are real, one has $f^{(-)}_{(e)l}(r, \lambda) = f^{(+)*}_{(e)l}(r, \lambda)$. For these new functions, at large distances, $r \gg a$, one has the asymptotics

$$f^{(+)}_{(e)l}(r, \lambda) \approx r^{-n/2} H^{(1)}_{\nu_l}(\lambda r), \quad f^{(-)}_{(e)l}(r, \lambda) \approx r^{-n/2} H^{(2)}_{\nu_l}(\lambda r), \qquad (4.4)$$

with $H^{(1,2)}_{\nu_l}(x)$ being the Hankel functions. Now it can be seen that the following identity takes place:

$$\frac{g_l(r, \lambda)g_l(r', \lambda)}{\bar{f}^{(1)2}_{(e)l}(a, \lambda) + \bar{f}^{(2)2}_{(e)l}(a, \lambda)}$$
$$= f^{(1)}_{(e)l}(r, \lambda)f^{(1)}_{(e)l}(r', \lambda)$$
$$-\frac{1}{2} \sum_{j=+,-} \frac{\bar{f}^{(1)}_{(e)l}(a, \lambda)}{\bar{f}^{(j)}_{(e)l}(a, \lambda)} f^{(j)}_{(e)l}(r, \lambda)f^{(j)}_{(e)l}(r', \lambda). \qquad (4.5)$$

By using the relation (4.5), the Wightman function from (4.2) can be written in the decomposed form:

$$W(x, x') = W_0(x, x') + W_c(x, x'), \qquad (4.6)$$

with the functions

$$W_0(x, x') = \sum_{l=0}^{\infty} \frac{l+n/2}{nS_D} C^{n/2}_l(\cos\theta)$$
$$\times \int_0^\infty d\lambda \frac{\lambda}{\omega} f^{(1)}_{(e)l}(r, \lambda)f^{(1)}_{(e)l}(r', \lambda)e^{-i\omega\Delta t}, \quad (4.7)$$

and

$$W_c(x, x') = -\sum_{l=0}^{\infty} \frac{l+n/2}{2nS_D} C^{n/2}_l(\cos\theta)$$
$$\times \sum_{j=+,-} \int_0^\infty d\lambda \frac{\lambda}{\omega} \frac{\bar{f}^{(1)}_{(e)l}(a, \lambda)}{\bar{f}^{(j)}_{(e)l}(a, \lambda)} f^{(j)}_{(e)l}(r, \lambda)f^{(j)}_{(e)l}(r', \lambda)$$
$$\times e^{-i\omega\Delta t}. \qquad (4.8)$$

The function $W_0(x, x')$ is the Wightman function in the case of the background when the geometry is described by the line element (2.3) for all values of the radial coordinate r. As a radial function in the corresponding modes, the function $f^{(1)}_{(e)l}(r, \lambda)$ is taken. Recall that we have $f^{(1)}_{(e)l}(r, \lambda) \approx r^{-n/2} J_{\nu_l}(\lambda r)$ for $r \to \infty$ and, hence, for these modes the vacuum state at asymptotic infinity coincides with the Minkowskian vacuum. Thus, the function $W_c(x, x')$ can be interpreted as the contribution to the Wightman function induced by the geometry in the region $r < a$ with the line element (2.1).

If bound states are present, the contribution of the corresponding modes to the Wightman function should be added to (4.6). For this contribution, by using the mode functions (3.29) with the normalization coefficient (3.39), in the exterior region we get

$$W_{\text{bs}}(x, x') = -\sum_{l=0}^{\infty} \frac{2l+n}{nS_D} C_l^{n/2}(\cos\theta) \sum_{\eta=\eta_s} \frac{\eta \hat{f}_{(eb)l}^{(1)}(a,\eta)}{\omega \partial_\eta \hat{f}_{(eb)l}^{(2)}(a,\eta)}$$
$$\times f_{(eb)l}^{(2)}(r,\eta) f_{(eb)l}^{(2)}(r',\eta) e^{-i\omega\Delta t}, \qquad (4.9)$$

where $\omega = \sqrt{m^2 - \eta^2}$ and $\eta = \eta_s$ are solutions of Eq. (3.31).

The part $W_c(x, x')$ of the Wightman function, induced by the interior geometry, can be further transformed by taking into account that, for large values of λ, for the functions $f_{(e)l}^{(j)}(r, \lambda)$ in (4.8), one has $f_{(e)l}^{(j)}(r, \lambda) \sim e^{ji\lambda r}$. By using this property and under the condition $|\Delta t| < (r + r' - 2a)$, assuming that the function $f_{(e)l}^{(+)}(r, \lambda)$ $(f_{(e)l}^{(-)}(r, \lambda))$ has no zeros for $0 < \arg\lambda < \pi/2$ $(-\pi/2 < \arg\lambda < 0)$, in (4.8) we can rotate the integration contour in the complex plane λ by the angle $\pi/2$ $(-\pi/2)$ for the term with $j = +$ $(j = -)$. In the presence of bound states, the integrands have simple poles at $\lambda = \eta_s e^{j\pi i/2}$, corresponding to the zeros of the function $\bar{f}_{(e)l}^{(j)}(a, \lambda)$ on the imaginary axis. These poles have to be circled on the right along contours with small radii. In the integrals over the imaginary axis $(\lambda = \eta e^{\pm i\pi/2})$, the integrands are expressed in terms of the functions $f_{(e)l}^{(1)}(a, \eta e^{\pm\pi i/2})$ and $f_{(e)l}^{(j)}(r, \eta e^{ji\pi/2})$, $j = +, -$. By comparing the asymptotics of the functions for $r \to \infty$, we can see that the functions $f_{(e)l}^{(j)}(r, \eta e^{j\pi i/2})$ are reduced to the function $f_{(eb)l}^{(2)}(r, \eta)$, up to a coefficient, and the function $f_{(e)l}^{(1)}(a, \eta e^{\pi i/2})$ is reduced to the function $f_{(eb)l}^{(1)}(a, \eta)$. By taking into account the normalization of the functions for large r and the relations between the Bessel functions and modified Bessel functions, we conclude that

$$f_{(e)l}^{(j)}(r, \eta e^{j\pi i/2}) = -j \frac{2i}{\pi} e^{-j\nu_l \pi i/2} f_{(eb)l}^{(2)}(r, \eta),$$
$$f_{(e)l}^{(1)}(a, \eta e^{j\pi i/2}) = e^{j\nu_l \pi i/2} f_{(eb)l}^{(1)}(a, \eta). \qquad (4.10)$$

By using these relations, one can see that the integrals over the regions $(0, im)$ and $(0, -im)$ cancel out, whereas the integrals over small semicircles around the poles $\eta_s e^{j\pi i/2}$ combine in the residue at the point $\eta_s e^{\pi i/2}$. An interesting fact is that the contribution of this residue to the part of the Wightman function (4.8) exactly cancels the corresponding contribution coming from the bound state [see (4.9)]. Finally, we get the following representation:

$$W_c(x, x') = -\sum_{l=0}^{\infty} \frac{2l+n}{\pi n S_D} C_l^{n/2}(\cos\theta) \int_m^{\infty} d\eta\eta \frac{\hat{f}_{(eb)l}^{(1)}(a,\eta)}{\hat{f}_{(eb)l}^{(2)}(a,\eta)}$$
$$\times \frac{\cosh(\Delta t \sqrt{\eta^2 - m^2})}{\sqrt{\eta^2 - m^2}} f_{(eb)l}^{(2)}(r,\eta) f_{(eb)l}^{(2)}(r',\eta).$$
$$(4.11)$$

Recall that, in deriving this formula we have assumed that $|\Delta t| < (r + r' - 2a)$. In particular, this condition is obeyed in the coincidence limit. An important advantage of the representation (4.11), compared with (4.8), is that in the upper limit of the integration the integrand decays exponentially instead of the strongly oscillatory behavior in (4.8).

With the known Wightman function, we can evaluate the VEVs of the field squared and the energy-momentum tensor by using the formulas below:

$$\langle 0|\varphi^2|0\rangle = \lim_{x' \to x} W(x, x'),$$
$$\langle 0|T_{ik}|0\rangle = \lim_{x' \to x} \partial_i \partial_k' W(x, x')$$
$$+ [(\xi - 1/4)g_{ik}\nabla_l\nabla^l - \xi\nabla_i\nabla_k - \xi R_{ik}]\langle 0|\varphi^2|0\rangle,$$
$$(4.12)$$

where R_{ik} is the Ricci tensor for the background spacetime. The expression for the energy-momentum tensor in (4.12) differs from the standard one, given, for example, in [17], by the term that vanishes on the mass shell (see [19]). Similarly to the Wightman function, the VEVs are decomposed into two parts:

$$\langle 0|\varphi^2|0\rangle = \langle\varphi^2\rangle_0 + \langle\varphi^2\rangle_c,$$
$$\langle 0|T_{ik}|0\rangle = \langle T_{ik}\rangle_0 + \langle T_{ik}\rangle_c, \qquad (4.13)$$

where the parts $\langle\varphi^2\rangle_0$ and $\langle T_{ik}\rangle_0$ are obtained from the Wightman function $W_0(x, x')$. The contributions $\langle\varphi^2\rangle_c$ and $\langle T_{ik}\rangle_c$ are induced by the geometry in the region $r < a$ and are given by formulas similar to (4.12) with $W(x, x')$ replaced by $W_c(x, x')$.

Of course, the coincidence limits in (4.12) are divergent and a renormalization procedure is necessary. An important point to be mentioned here is that, for points $r > a$ the local geometry is not changed by the interior region and, as a consequence, the divergences are contained in the parts $\langle\varphi^2\rangle_0$ and $\langle T_{ik}\rangle_0$ and the parts $\langle\varphi^2\rangle_c$ and $\langle T_{ik}\rangle_c$ are finite. Hence, providing an explicit decomposition of the Wightman function in the form (4.11), we have reduced the renormalization procedure for the VEVs to the one in the case of the background where the geometry is described by the line element (2.3) for all values of the radial coordinate r.

In particular, by taking into account that

$$C_l^{n/2}(1) = \frac{\Gamma(l+n)}{\Gamma(n)\Gamma(l+1)}, \qquad (4.14)$$

for the contribution in the VEV of the field squared induced by the interior geometry we get the expression

$$\langle \varphi^2 \rangle_c = -\frac{\Gamma(D/2)}{2\pi^{D/2+1}} \sum_{l=0}^{\infty} D_l \int_m^{\infty} d\eta \, \frac{\hat{f}_{(eb)l}^{(1)}(a,\eta)}{\hat{f}_{(eb)l}^{(2)}(a,\eta)} \frac{\eta f_{(eb)l}^{(2)2}(r,\eta)}{\sqrt{\eta^2 - m^2}},$$

(4.15)

where

$$D_l = \frac{(2l+n)\Gamma(l+n)}{\Gamma(D-1)\Gamma(l+1)} \tag{4.16}$$

is the degeneracy of the angular mode with a given l. The corresponding VEV of the energy-momentum tensor is obtained from (4.12). The VEV (4.15), in general, diverges on the boundary $r = a$. The leading term of the corresponding asymptotic expansion over the distance from the boundary depends on the specific interior and exterior geometries and examples will be done below.

We have considered the Wightman function in the exterior region. The mode sum for the corresponding function in the interior region is obtained by using the interior modes from (3.14) with the normalization coefficient (3.21). Subtracting from the mode sum the Wightman function for the geometry described by the line element (2.1) for all values of the radial coordinate, we can separate the part induced by the exterior geometry. In what follows we will be concerned with the VEVs in the exterior region.

V. MINKOWSKI SPACETIME AS AN EXTERIOR GEOMETRY

A. Wightman function

As an application of general results given in previous sections, here we assume that the exterior geometry is described by the Minkowski spacetime. The corresponding line element has the form

$$ds_e^2 = dt^2 - dr^2 - r^2 d\Omega_{D-1}^2, \tag{5.1}$$

with the functions appearing in (2.3):

$$u_e(r) = v_e(r) = 0, \qquad e^{w_e(r)} = r. \tag{5.2}$$

In this case, in the exterior region we have the radial functions

$$f_{(e)l}^{(1)}(r,\lambda) = r^{-n/2} J_{\nu_l}(\lambda r), \qquad f_{(e)l}^{(2)}(r,\lambda) = r^{-n/2} Y_{\nu_l}(\lambda r),$$
$$f_{(e)l}^{(+)}(r,\lambda) = r^{-n/2} H_{\nu_l}^{(1)}(\lambda r), \qquad f_{(e)l}^{(-)}(r,\lambda) = r^{-n/2} H_{\nu_l}^{(2)}(\lambda r).$$

(5.3)

For the corresponding functions on the imaginary axis, we get

$$f_{(eb)l}^{(1)}(r,\eta) = r^{-n/2} I_{\nu_l}(\eta r),$$
$$f_{(eb)l}^{(2)}(r,\eta) = r^{-n/2} K_{\nu_l}(\eta r). \tag{5.4}$$

In the special case under consideration, $W_0(x,x')$ is the Wightman function in the Minkowski spacetime. For the contribution induced by the interior geometry, we have the expression

$$W_c(x,x') = -\sum_{l=0}^{\infty} \frac{(2l+n)C_l^{n/2}(\cos\theta)}{\pi n S_D (rr')^{n/2}}$$
$$\times \int_m^{\infty} d\eta \, \frac{\tilde{I}_{\nu_l}(\eta a)}{\tilde{K}_{\nu_l}(\eta a)}$$
$$\times \frac{\cosh(\Delta t \sqrt{\eta^2 - m^2})}{\sqrt{\eta^2 - m^2}} K_{\nu_l}(\eta r) K_{\nu_l}(\eta r'). \tag{5.5}$$

In this formula, for a given function $F(z)$ we have defined

$$\tilde{F}(z) = zF'(z) - \left[ay_l(a,\eta) + \frac{16\pi G\xi}{D-1}\tau a + \frac{D}{2} - 1\right] F(z), \tag{5.6}$$

with the notation

$$y_l(r,\eta) = \frac{\partial_r f_{(i)l}^{(1)}(r,i\eta)}{f_{(i)l}^{(1)}(r,i\eta)}, \tag{5.7}$$

and with

$$\frac{8\pi G}{D-1}\tau = u_i'(a) + (D-1)[w_i'(a) - 1/a]. \tag{5.8}$$

Note that, for the exterior Minkowskian spacetime, Eq. (3.31), defining the bound states, is written in the form

$$\tilde{K}_{\nu_l}(\eta a) = 0, \qquad \eta < m. \tag{5.9}$$

The existence of the solutions for this equation with $\eta > m$ leads to the instability of the exterior Minkowskian vacuum. An example of this type will be discussed below in Sec. VI.

The expression (5.5) differs from the corresponding formula for the Wightman function outside a spherical boundary in Minkowski spacetime with the Robin boundary condition $(\beta_R + \partial_r)\varphi = 0$ at $r = a$ (see [20]) by the replacement of the Robin coefficient:

$$\beta_R \rightarrow -y_l(a,\eta) - \frac{16\pi G\xi}{D-1}\tau. \tag{5.10}$$

In the problem under consideration, the effective Robin coefficient depends on both η and l. As it will be shown below, this leads to the weakening of divergences in the local VEVs on the boundary.

B. VEV of the field squared

The renormalization of the VEVs in the exterior region is reduced to the subtraction of the corresponding VEVs in

Minkowski spacetime. In this case the renormalized VEVs of the field squared and the energy-momentum tensor coincide with the parts $\langle \varphi^2 \rangle_c$ and $\langle T_{ik} \rangle_c$ induced by the interior geometry. For the renormalized VEV of the field squared, we get

$$\langle \varphi^2 \rangle_c = -\frac{\Gamma(D/2)}{2\pi^{D/2+1}r^{D-2}}\sum_{l=0}^{\infty}D_l\int_m^\infty d\eta\eta\frac{\tilde{I}_{\nu_l}(a\eta)}{\tilde{K}_{\nu_l}(a\eta)}\frac{K_{\nu_l}^2(r\eta)}{\sqrt{\eta^2-m^2}}.$$

(5.11)

Let us discuss the behavior of this VEV in the asymptotic regions of the parameters.

At large distances from the boundary and for a massive field, assuming that $mr \gg 1$ for a fixed ma, the dominant contribution to the integral in (5.11) comes from the region near the lower limit of the integration. By using the asymptotic formula for the Macdonald function for large values of the argument, to the leading order we get

$$\langle \varphi^2 \rangle_c \approx -\frac{\Gamma(D/2)e^{-2rm}}{8\pi^{(D+1)/2}\sqrt{mr}r^{D-1}}\sum_{l=0}^{\infty}D_l\frac{\tilde{I}_{\nu_l}(am)}{\tilde{K}_{\nu_l}(am)}.$$

(5.12)

Hence, at distances from the boundary larger than the Compton wavelength, the VEV is exponentially suppressed. For a massless field and for $r \gg a$, we introduce in (5.11) a new integration variable $y = r\eta$ and expand the functions $\tilde{I}_{\nu_l}(ya/r)$ and $\tilde{K}_{\nu_l}(ya/r)$. The contribution of the leading term for a given l behaves as $(a/r)^{2l+2D-3}$ and the integral is evaluated by using the formula

$$\mathcal{I}(\nu) \equiv \int_0^\infty dy\, y^{2\nu}K_\nu^2(y) = \frac{\pi\Gamma(2\nu+1/2)\Gamma(\nu+1/2)}{4\Gamma(\nu+1)}.$$

(5.13)

The dominant contribution comes from the term with the lowest orbital momentum $l=0$ with the leading term

$$\langle \varphi^2 \rangle_c \approx \frac{D/2-1-\beta_0}{D/2-1+\beta_0}\frac{(D-2)\Gamma(D-3/2)\Gamma((D-1)/2)}{2(4\pi)^{D/2}\Gamma^2(D/2)a^{D-1}}$$
$$\times (a/r)^{2D-3},$$

(5.14)

where

$$\beta_0 = ay_0(a,0) + \frac{16\pi G\xi}{D-1}\tau a + \frac{D}{2} - 1.$$

(5.15)

If $\beta_0 = D/2 - 1$ or $\beta_0 = 1 - D/2$, the next-to-leading order terms should be kept in the expansions of the functions $\tilde{I}_{\nu_l}(ya/r)$ and $\tilde{K}_{\nu_l}(ya/r)$, respectively. Hence, for a massless field the decay of the VEV at large distances follows a power law.

The VEV of the field squared (5.11) diverges on the boundary $r = a$. The surface divergences in the VEVs of local physical observables are well known in the theory of the Casimir effect and were investigated for various types of boundary geometries. In the problem at hand, the

appearance of divergences is related to the idealized model of the zero thickness transition range between the interior and exterior geometries. In order to find the leading term in the asymptotic expansion over the distance from the boundary, we note that for points near the boundary the dominant contribution to the series in (5.11) comes from large values of l. For these l, introducing a new integration variable $x = a\eta/\nu_l$, we use the uniform asymptotic expansions for the modified Bessel functions for large values of the order (see, for instance, [21]). For the further evaluation we also need the uniform asymptotic expansion of the function $y_l(r, \eta)$. From Eq. (3.8) for the interior radial mode function the following equation for the function (5.7) is obtained:

$$y_l'(r,\eta) + y_l^2(r,\eta) + [u_i' - v_i' + (D-1)w_i']y_l(r,\eta)$$
$$- e^{2v_i}\left[\frac{\eta^2-m^2}{e^{2u_i}} + m^2 + \xi R_{(i)} + \frac{l(l+n)}{e^{2w_i}}\right] = 0. \quad (5.16)$$

From here it follows that for the leading term in the asymptotic expansion of the function $y_l(r, \nu_l x)$ for large values of l one has

$$y_l(r, \nu_l x) \approx \pm\nu_l e^{v_i}\sqrt{e^{-2u_i}x^2 + e^{-2w_i}}.$$

(5.17)

For the function $f_{(i)l}(r, i\eta)$ in (5.7), regular at the center, the upper sign should be taken. By taking into account that $u_i(a) = v_i(a) = 0$ and $e^{2w_i(a)} = a^2$, the asymptotic expansion at $r = a$ can be written as

$$y_l(a, \nu_l x) \approx \frac{\nu_l}{a}\sqrt{a^2x^2 + 1}\left[1 + \frac{B(ax)}{\nu_l} + \cdots\right],$$

(5.18)

where the function $B(ax)$ depends on the interior geometry.

By making use of the uniform asymptotic expansions for the modified Bessel functions, with the combination of (5.18), we can see that the leading order contribution to the function $\tilde{I}_{\nu_l}(\nu_l x)$ coming form the first term in (5.18) is canceled by the leading term in the asymptotic expansion of the function $zI_{\nu_l}'(z)$ with $z = \nu_l x$. As a result, for the ratio appearing in (5.11), in the leading order, we get

$$\frac{\tilde{I}_{\nu_l}(\nu_l x)}{\tilde{K}_{\nu_l}(\nu_l x)} \approx \frac{C(x)}{2\pi l}e^{2l\eta(x)},$$

(5.19)

with the function

$$C(x) = B(x) + \left(\frac{16\pi G\xi}{D-1}\tau a + \frac{D}{2} - 1\right)\frac{1}{\sqrt{1+x^2}} + \frac{x^2/2}{(1+x^2)^{3/2}},$$

(5.20)

and with the standard notation (see [21])

$$\eta(x) = \sqrt{1 + x^2} + \ln\frac{x}{1 + \sqrt{1 + x^2}}. \tag{5.21}$$

The function $B(x)$ for special cases of the interior dS and AdS spaces will be given below.

Substituting (5.19) and the uniform asymptotic expansion for the function $K_{\nu_l}^2(\nu_l xr/a)$ into (5.11), with a new integration variable $x = a\eta/\nu_l$, in the leading order we use the relations $D_l \approx 2l^{D-2}/\Gamma(D-1)$ and $\eta(xr/a) - \eta(x) \approx \sqrt{1 + x^2}(r/a - 1)$. In the same order, by taking into account that $\sum_{l=0}^{\infty} l^{p-1} e^{-\alpha l} \approx \Gamma(p)/\alpha^p$ for $\alpha \to 0$, for the leading term in the asymptotic expansion of the VEV for the field squared near the boundary one gets

$$\langle\varphi^2\rangle_c \approx -\frac{\Gamma(D/2)(r-a)^{2-D}}{2^D(D-2)\pi^{D/2+1}a}\int_0^{\infty} dx\frac{C(x)}{(1 + x^2)^{(D-1)/2}}. \tag{5.22}$$

Note that for a spherical boundary in Minkowski spacetime on which the field operator obeys Dirichlet or Neumann (or, in general, Robin) boundary conditions, the VEV of the field squared diverges on the boundary as $(r-a)^{1-D}$ and the divergence is stronger.

C. Vacuum energy-momentum tensor

The VEV of the energy-momentum tensor is evaluated by using the formula (4.12). The renormalization in the exterior region is reduced to the subtraction of the part that corresponds to the Minkowski spacetime for all $0 \le r < \infty$. The VEV of the energy-momentum tensor is diagonal. For the renormalized components we get (with no summation over i)

$$\langle T_i^i\rangle_c = \frac{\Gamma(D/2)}{4\pi^{D/2+1}r^D}\sum_{l=0}^{\infty} D_l \int_m^{\infty} d\eta\eta\frac{\tilde{I}_{\nu_l}(a\eta)}{\tilde{K}_{\nu_l}(a\eta)}\frac{G_{\nu_l}^{(i)}[K_{\nu_l}(r\eta)]}{\sqrt{\eta^2 - m^2}}, \tag{5.23}$$

where for a given function $f(y)$ we define

$$G_\nu^{(0)}[f(y)] = (4\xi - 1)\left[y^2 f'^2(y) - nyf(y)f'(y) + \left(\nu^2 - \frac{(1+4\xi)y^2 - 2(mr)^2}{1 - 4\xi}\right)f^2(y)\right],$$

$$G_\nu^{(1)}[f(y)] = y^2 f'^2(y) + \xi_1 yf(y)f'(y) - (y^2 + \nu^2 + \xi_1 n/2)f^2(y),$$

$$G_\nu^{(j)}[f(y)] = (4\xi - 1)y^2 f'^2(y) - \xi_1 yf(y)f'(y) + \left[(4\xi - 1)y^2 + \frac{\nu^2(1 + \xi_1) + \xi_1 n/2}{n + 1}\right]f^2(y), \tag{5.24}$$

with $j = 2, ..., D$. In (5.24), the notation

$$\xi_1 = (D - 1)(4\xi - 1) + 1 \tag{5.25}$$

is introduced. In general, the vacuum stresses along the radial and azimuthal directions are isotropic.

It can be checked that the VEV given by (5.23) obeys the covariant conservation equation $\nabla_k\langle T_i^k\rangle_c = 0$, which, for the geometry under consideration, is reduced to a single equation:

$$r\partial_r\langle T_1^1\rangle_c + (D - 1)(\langle T_1^1\rangle_c - \langle T_2^2\rangle_c) = 0. \tag{5.26}$$

We also have a trace relation:

$$\langle T_i^i\rangle_c = [D(\xi - \xi_D)\nabla_l\nabla^l + m^2]\langle\varphi^2\rangle_c. \tag{5.27}$$

In particular, the vacuum energy-momentum tensor is traceless for a conformally coupled massless scalar field.

Now let us investigate the behavior of the vacuum energy-momentum tensor at large distances and near the boundary. At large distances from the sphere and for a massive field, similarly to (5.12), in the leading order we get

$$\langle T_0^0\rangle_c \approx \langle T_2^2\rangle_c \approx -\frac{2mr}{D - 1}\langle T_1^1\rangle_c$$

$$\approx \frac{\Gamma(D/2)m^2(\xi - 1/4)}{2\pi^{(D-1)/2}r^{D-1}\sqrt{mr}e^{2mr}}\sum_{l=0}^{\infty} D_l\frac{\tilde{I}_{\nu_l}(am)}{\tilde{K}_{\nu_l}(am)}. \tag{5.28}$$

Note that in this region $|\langle T_1^1\rangle_c| \ll |\langle T_0^0\rangle_c|$. For a massless field, assuming that $r \gg a$, we introduce a new integration variable, $y = r\eta$, in (5.23) and expand the integrand over a/r. For a given l, the leading term behaves like $(a/r)^{2l+2D-1}$ and it contains the integrals $\int_0^{\infty} dy y^{2\nu_l+2} F_{\nu_l}^{(i)}[K_{\nu_l}(y)]$. These integrals are evaluated by using the relations

$$\int_0^{\infty} dy y^{2\nu+1} K_\nu(y)K_\nu'(y) = -(\nu + 1/2)\mathcal{I}(\nu),$$

$$\int_0^{\infty} dy y^{2\nu+2} K_\nu'^2(y) = \left[\nu^2 + (\nu + 1/4)\frac{\nu + 3/2}{\nu + 1}\right]\mathcal{I}(\nu), \tag{5.29}$$

with the function $\mathcal{I}(\nu)$ defined by (5.13). These relations are proved by making use of the well-known properties of the Macdonald functions. The dominant contributions come from the terms with $l = 0$ and, to the leading order, for the energy density we find

$$\langle T_0^0 \rangle_c \approx -\frac{(\xi - \xi_D)(a/r)^{2D-1}}{2^{D-2}\pi^{D/2}a^{D+1}}\frac{D/2 - 1 - \beta_0}{D/2 - 1 + \beta_0}$$
$$\times \frac{\Gamma(D - 1/2)\Gamma((D+1)/2)}{\Gamma(D/2)\Gamma(D/2 - 1)}. \qquad (5.30)$$

The asymptotics of the radial and azimuthal stresses are given by the relations

$$\langle T_1^1 \rangle_c \approx -\frac{D-1}{D}\langle T_2^2 \rangle_c \approx -\langle T_0^0 \rangle_c. \qquad (5.31)$$

As is seen, for a massless field, at large distances from the boundary the radial pressure, $-\langle T_1^1 \rangle_c$, is equal to the energy density. For a conformally coupled field, the leading terms vanish.

The asymptotic behavior of the VEV of the energy-momentum tensor near the boundary $r = a$ is investigated in a way similar to what we used for the field squared. By using (5.19) and the uniform asymptotic expansions for the Macdonald function and its derivative, in the leading order we obtain

$$\langle T_0^0 \rangle_c \approx \frac{(D-1)\Gamma(D/2)}{2^{D+2}\pi^{D/2+1}a(r-a)^D}\int_0^\infty dx\frac{4\xi(x^2+1)-1}{(x^2+1)^{(D+1)/2}}C(x),$$

$$\langle T_2^2 \rangle_c \approx \frac{(D-1)\Gamma(D/2)}{2^{D+2}\pi^{D/2+1}a(r-a)^D}\int_0^\infty dx\frac{C(x)}{(1+x^2)^{(D+1)/2}}$$
$$\times \left[(4\xi - 1)(x^2 + 1) + \frac{1}{D-1}\right], \qquad (5.32)$$

where the function $C(x)$, defined by (5.20), depends on the specific geometry in the region $r < a$. The leading term in the asymptotic expansion of the radial stress is most easily found by making use of the continuity equation (5.26):

$$\langle T_1^1 \rangle_c \approx -\frac{r-a}{a}\langle T_2^2 \rangle_c. \qquad (5.33)$$

For a spherical boundary in Minkowski spacetime with Dirichlet or Neumann boundary conditions on the field operator, the leading terms have the form (with no summation over i)

$$\langle T_i^i \rangle_c \approx \pm\frac{2D\Gamma((D+1)/2)}{(4\pi)^{(D+1)/2}(r-a)^{D+1}}(\xi - \xi_D), \qquad (5.34)$$

for $i = 0, 2, \ldots, D$, and for the radial stress one has

$$\langle T_1^1 \rangle_c \approx -\frac{D-1}{D}(r/a - 1)\langle T_2^2 \rangle_c. \qquad (5.35)$$

In (5.34), the upper/lower sign corresponds to the Dirichlet/Neumann boundary condition. The leading terms for the case of the Robin boundary condition coincide with those for the Neumann condition. Similarly

to the case of the field squared, the divergences in these cases are stronger compared to those for the geometry under consideration.

VI. EXAMPLES OF THE INTERIOR METRIC: dS AND AdS SPACES

In this section, as examples of the interior metric we consider the maximally symmetric spacetimes with positive and negative cosmological constants, namely, dS and AdS spaces. As in the previous section, the exterior geometry is described by the Minkowski spacetime with the exterior line element (5.1). For the interior dS and AdS spaces, the corresponding line element in static coordinates has the form

$$ds_i^2 = (1 + k\tilde{r}^2/\alpha^2)d\tilde{t}^2 - (1 + k\tilde{r}^2/\alpha^2)^{-1}d\tilde{r}^2 - \tilde{r}^2d\Omega_{D-1}^2, \qquad (6.1)$$

where $k = -1$ and $k = 1$ for dS and AdS spaces, respectively. The parameter α is related to the cosmological constant Λ through the expression $\alpha = D(D-1)/(2|\Lambda|)$. In the case of dS space we assume that the boundary is inside the dS horizon, corresponding to $\tilde{r} = \alpha$.

We should transform the line element in the form that is continuously glued with the exterior Minkowskian line element at the boundary. To this aim, first we introduce a new radial coordinate, r, in accordance with

$$\tilde{r} = \alpha S_k(x), \qquad x = (r - r_c)/\alpha, \qquad (6.2)$$

where $r_c \leq r \leq a$ and

$$S_k(x) = \begin{cases} \sin x, & k = -1 \\ \sinh x, & k = 1 \end{cases}. \qquad (6.3)$$

The parameter r_c will be determined below by the matching conditions on the boundary. Note that in the case of dS space the horizon corresponds to $x = \pi/2$ and, hence, to the value of the new radial coordinate $r = \pi\alpha/2 + r_c$. With the coordinate transformation (6.2), the line element takes the form

$$ds_i^2 = C_k^2(x)d\tilde{t}^2 - dr^2 - \alpha^2 S_k^2(x)d\Omega_{D-1}^2, \qquad (6.4)$$

where

$$C_k(x) = \begin{cases} \cos x, & k = -1 \\ \cosh x, & k = 1 \end{cases}. \qquad (6.5)$$

Now the component g_{11} of the metric tensor is continuous at $r = a$. From (6.4) it follows that the coordinate r measures the proper distance along the radial direction.

Next, we define a new time coordinate, t, in accordance with

$$\tilde{t} = \frac{t}{C_k(x_a)}, \qquad x_a = \frac{a - r_c}{\alpha}. \tag{6.6}$$

For the interior line element, we get

$$ds_i^2 = \frac{C_k^2(x)}{C_k^2(x_a)} dt^2 - dr^2 - \alpha^2 S_k^2(x) d\Omega_{D-1}^2. \tag{6.7}$$

In terms of the new coordinate t, at the boundary, the component g_{00} is continuous as well. From (6.7), for the interior functions in (2.1), one finds

$$e^{u_i(r)} = \frac{C_k(x)}{C_k(x_a)}, \quad v_i(r) = 0, \quad e^{w_i(r)} = \alpha S_k(x), \tag{6.8}$$

with x given by (6.2).

The metric tensor corresponding to (6.7) should be glued at $r = a$ with the exterior Minkowski spacetime in spherical coordinates with the line element (5.1) and with the functions (5.2). As we have already noticed, the components g_{00} and g_{11} are continuous. From the continuity of the components g_{ll}, $l = 2, \ldots, D$, we get

$$S_k(x_a) = a/\alpha, \tag{6.9}$$

with x_a defined by (6.6). For a given a and α, Eq. (6.9) determines the value of the parameter r_c. For dS space, r_c is negative $(1 - \pi/2 \leq r_c < 0$ for $0 \leq a/\alpha < 1)$ and for AdS space it is positive. In the latter case and for large values of a/α one has $r_c/\alpha \approx a/\alpha - \ln(2a/\alpha)$. From (6.9) it follows that for the dS space the boundary near the dS horizon $(x_a \to \pi/2)$ corresponds to the limit $a \to \alpha$. Note that, by taking into account (6.9), for $C_k(x_a)$ in (6.7) one obtains

$$C_k(x_a) = \sqrt{1 + k(a/\alpha)^2}. \tag{6.10}$$

For the components of the surface energy-momentum tensor, from (2.9), we get the expressions (with no summation over i)

$$\tau_0^0 = \frac{D-1}{8\pi G a}[C_k(x_a) - 1],$$

$$\tau_i^i = \frac{D-2}{8\pi G a}\left[\frac{ka^2/\alpha^2}{(D-2)C_k(x_a)} + C_k(x_a) - 1\right], \tag{6.11}$$

with $i = 2, \ldots, D$. Note that the surface energy density is negative for the interior dS space and is positive for the AdS space. In the case of dS space, one has $C_k(x_a) \to 0$ in the limit; then the boundary tends to the dS horizon, $a \to \alpha$. In this limit, the azimuthal stress in (6.11) diverges.

With the line element (6.7), Eq. (3.8) for the interior radial functions takes the form

$$\frac{\partial_x[C_k(x)S_k^{D-1}(x)\partial_x f_{(i)l}(r)]}{C_k(x)S_k^{D-1}(x)} + \left[\frac{\alpha^2\omega^2 C_k^2(x_a)}{C_k^2(x)} - \frac{l(l+D-2)}{S_k^2(x)}\right.$$

$$\left. - \alpha^2(m^2 + \xi R_{(i)})\right] f_{(i)l}(r) = 0, \tag{6.12}$$

where the Ricci scalar is given by

$$R_{(i)} = -kD(D+1)/\alpha^2. \tag{6.13}$$

The solution of Eq. (6.12), regular at the center, $x = 0$, is expressed in terms of the hypergeometric function as (see also [22])

$$f_{(i)l}^{(1)}(r, \lambda) = \frac{[\tanh(\sqrt{k}x)/\sqrt{k}]^l}{\cosh^{D/2+\nu}(\sqrt{k}x)} F(b_{l\lambda}^{(+)}, b_{l\lambda}^{(-)};$$

$$l + D/2; \tanh^2(\sqrt{k}x)), \tag{6.14}$$

where we have introduced the notations

$$\nu = \sqrt{D^2/4 + k\alpha^2 m^2 - D(D+1)\xi},$$

$$b_{l\lambda}^{(\pm)} = \frac{1}{2}[l + D/2 + \nu \pm \sqrt{k}\alpha C_k(x_a)\sqrt{\lambda^2 + m^2}]. \tag{6.15}$$

For the dS interior, the parameter ν can be either real or purely imaginary. In the AdS case and for the imaginary ν the ground state becomes unstable [23,24]. By using formula 9.1.70 from [21], it can be seen that in the limit $\alpha \to \infty$ the function $f_{(i)l}^{(1)}(r, \lambda)$ reduces to the function $r^{-n/2}J_{\nu_l}(\lambda r)$, up to a constant coefficient. Note that in the expressions of the VEVs in the exterior region the function (6.14) enters in the form (5.7) and, hence, the coefficient is not relevant. The second linearly independent solution of (6.12) is given by the expression

$$f_{(i)l}^{(2)}(r, \lambda) = \frac{[\sqrt{k}\coth(\sqrt{k}x)]^{l+D-2}}{\cosh^{D/2-\nu}(\sqrt{k}x)} F(1 - b_{l\lambda}^{(+)}, 1 - b_{l\lambda}^{(-)};$$

$$2 - l - D/2; \tanh^2(\sqrt{k}x)). \tag{6.16}$$

By using the relation [21]

$$F(a, b; c; z) = (1 - z)^{c-a-b}F(c - a, c - b; c; z), \tag{6.17}$$

for the hypergeometric function, we can see that the solutions (6.14) and (6.16) are symmetric under the change $\nu \to -\nu$. In particular, from here it follows that these solutions are real for purely imaginary values of ν. We also have the property $f_{(i)l}^{(j)}(r, \lambda e^{\pi i}) = f_{(i)l}^{(j)}(r, \lambda)$, $j = 1, 2$.

Now, the Wightman function and the VEVs of the field squared and of the energy-momentum tensor in the exterior region are given by Eqs. (5.5), (5.11), and (5.23), where now in the definition (5.6) one has

$$\frac{8\pi G}{D-1}\tau a = \frac{ka^2/\alpha^2}{C_k(x_a)} + (D-1)[C_k(x_a) - 1]. \quad (6.18)$$

In the expression of the logarithmic derivative of the radial function (6.14) we use the following formula for the derivative of the hypergeometric function:

$$(c-n)_n z^{c-1-n} F(a,b;c-n;z) = \partial_z^n [z^{c-1} F(a,b;c;z)], \quad (6.19)$$

where $(c)_n$ is Pochhammer's symbol. Taking $n = 1$, we get

$$\frac{\partial_z F(a,b;c;z)}{F(a,b;c;z)} = \frac{c-1}{z}\left[\frac{F(a,b;c-1;z)}{F(a,b;c;z)} - 1\right]. \quad (6.20)$$

With the help of this formula, the expression of the logarithmic derivative for the radial function (6.14) is presented in the form

$$\frac{\partial_r f_{(i)l}^{(1)}(r,\lambda)}{f_{(i)l}^{(1)}(r,\lambda)} = \frac{1}{\alpha\sqrt{kz}}\left\{l - (\nu_l + \nu + 1)z + 2(1-z)\nu_l\right.$$
$$\left. \times\left[\frac{F(b_{l\lambda}^{(+)}, b_{l\lambda}^{(-)}; \nu_l; z)}{F(b_{l\lambda}^{(+)}, b_{l\lambda}^{(-)}; \nu_l + 1; z)} - 1\right]\right\}, \quad (6.21)$$

with the notation

$$z = \tanh^2(\sqrt{k}x), \quad (6.22)$$

and with x defined in (6.2).

In the expression of the VEVs in the exterior region, the logarithmic derivative (6.21) is evaluated at $r = a$. In this case

$$z|_{r=a} = z_a = \frac{1}{1 + k\alpha^2/a^2}, \quad (6.23)$$

and in the notation (5.6) with a tilde, one has

$$y_l(a,\eta) = \frac{(kz_a)^{-1/2}}{\alpha}\{l - (\nu_l + \nu + 1)z_a$$
$$+ 2(1-z_a)\nu_l[F_{\nu_l}(\eta, z_a) - 1]\}. \quad (6.24)$$

Here, we have defined the function

$$F_{\nu_l}(\eta, z_a) = \frac{F(b_l^+(\eta), b_l^-(\eta); \nu_l; z_a)}{F(b_l^+(\eta), b_l^-(\eta); \nu_l + 1; z_a)}, \quad (6.25)$$

with

$$b_l^\pm(\eta) = \frac{1}{2}\left[\nu_l + \nu + 1 \pm i\sqrt{k}\alpha C_k(x_a)\sqrt{\eta^2 - m^2}\right] \quad (6.26)$$

and with $C_k(x_a)$ given by (6.10). Hence, for the interior dS and AdS geometries, the VEVs of the field squared and the energy-momentum tensor in the exterior Minkowskian

region are given by (5.11) and (5.23), where in the expressions for $\tilde{I}_{\nu_l}(a\eta)$ and $\tilde{K}_{\nu_l}(a\eta)$, defined by (5.6), we should substitute (6.18) and (6.24).

The equation for bound states is obtained from (5.9) with the same substitutions. By a numerical calculation, we have seen that, for a given $a\eta$, the function $|\tilde{K}_{\nu_l}(a\eta)|$ increases with increasing l and, hence, if there are no bound states for $l = 0$ the same will be the case for a higher l. For the interior AdS geometry, the function $\tilde{K}_{\nu_l}(a\eta)$ is always negative and in this case there are no bound states. For the dS interior the same is the case for a minimally coupled field. The situation is changed in the case of dS interior geometry for nonminimally coupled fields. We will discuss the features on the example of a conformally coupled field.

If the dS horizon is not too close to the separating boundary, once again, the function $\tilde{K}_{\nu_l}(a\eta)$ is negative and the bound states are absent. However, bound states appear for $\alpha = \alpha_1 > a$, where α_1 is some critical value sufficiently close to a. With a further decrease of α, the value of $a\eta$ corresponding to the bound state increases and, starting from the second critical value $\alpha = \alpha_2$, it becomes larger than ma. This corresponds to the imaginary value of the energy for the mode and signals the instability of the exterior Minkowskian vacuum for $a < \alpha < \alpha_2$. For a massless field, any possible real solution of the equation $\tilde{K}_{\nu_l}(a\eta) = 0$ leads to the instability of the exterior vacuum. We have illustrated this type of situation for dS space in Fig. 1, where for $l = 0$ the function $\tilde{K}_{\nu_l}(a\eta)$ is plotted versus $a\eta$ for a conformally coupled scalar field in $D = 3$ spatial dimensions. For the left panel, we have taken $ma = 1/4$ and the right panel is for a massless field. The curves on the left panel correspond to the values of the ratio $\alpha/a = 1.0018, 1.0025, 1.00281, 1.0035, 1.005$, increasing from top to bottom lines. For the first critical value, corresponding to the appearance of the bound state, one has $\alpha_1/a \approx 1.00281$. The second critical value, starting from which the vacuum becomes unstable, corresponds to $\alpha_2/a \approx 1.0021$. The left zero on the left panel corresponds to a bound state ($\eta_s < m$), whereas the right zero corresponds to an unstable mode ($\eta_s > m$). For the curves on the right panel, we have $\alpha/a = 1.002, 1.0025, 1.00305, 1.005, 1.1$ (increasing from top to bottom lines). Here, any solution of Eq. (5.9) corresponds to the instability, and for the critical value of the dS curvature radius we have $\alpha_2/a \approx 1.00305$.

Now we turn to the investigation of the asymptotic behavior of the VEVs. At large distances, the asymptotics are given by (5.12), (5.28), and (5.14), (5.30) for massive and massless fields, respectively. For the interior geometries under consideration, the quantity β_0, appearing in the asymptotic for a massless field, is given by the expression

$$\beta_0 = \frac{1}{C_k(x_a)}\{2k(a/\alpha)^2(\xi - b_0) + n[F(z_a) - 1]\}$$
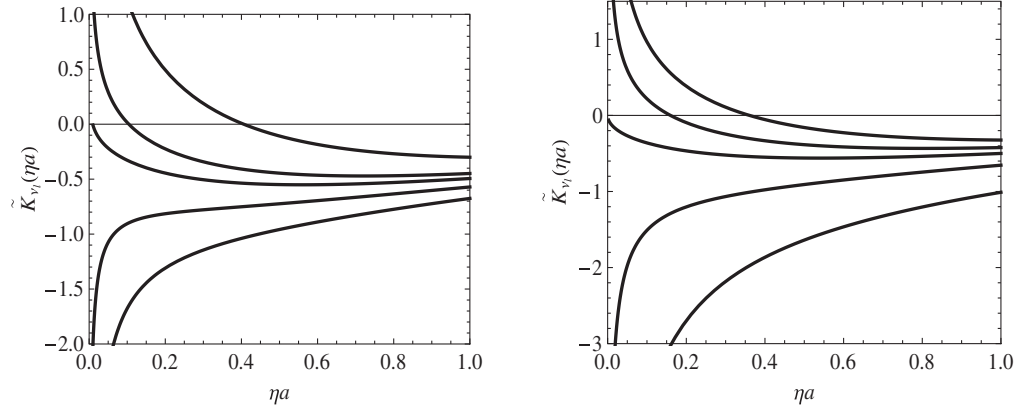$$+ 2\xi(D-1)[C_k(x_a) - 1] + n/2, \quad (6.27)$$

FIG. 1.   The function $\tilde{K}_{\nu_l}(a\eta)$ in the equation of the bound states for $l = 0$ versus $a\eta$ in the case of a conformally coupled field in $D = 3$ spatial dimensions. The left panel corresponds to a massive field with $ma = 1/4$ and the right panel presents the case of a massless field. For the graphs on the left panel, $\alpha/a = 1.0018, 1.0025, 1.00281, 1.0035, 1.005$, and, for the right panel, $\alpha/a = 1.002, 1.0025, 1.00305, 1.005, 1.1$ (increasing from top to bottom lines in both cases).

where $b_0 = D/4 + \nu/2$ and we have defined the function

$$F(z_a) = \frac{F(b_0, b_0; D/2 - 1; z_a)}{F(b_0, b_0; D/2; z_a)}. \qquad (6.28)$$

For a minimally coupled field, for this function one has

$$F(z_a) = 1 + \frac{kD}{D-2}\frac{a^2}{\alpha^2}, \qquad (6.29)$$

and from (6.27) we get $\beta_0 = D/2 - 1$. Now, from (5.14) and (5.30), we see that the leading terms in the asymptotic expansion of the VEVs at large distances vanish and the decay for this case is stronger. For a conformally coupled field and for $D = 3$, one has $b_0 = 1$, and the function $F(z)$ in (6.28) is reduced to

$$F(z_a) = k\frac{a^2}{\alpha^2} + \frac{a/\alpha}{A_k(1/\sqrt{\alpha^2/a^2 + k})}, \qquad (6.30)$$

with

$$A_k(x) = \begin{cases} \text{arcsinh}x, & k = -1 \\ \arcsin x, & k = 1 \end{cases}. \qquad (6.31)$$

With the function (6.30) in (6.27), one has $(n - 2\beta_0)/(n + 2\beta_0) > 0$ for all values of a/α in the AdS case and for $a/\alpha < a/\alpha_2$ for the dS interior. In the latter case $a/\alpha_2 \approx 0.997$ is the critical value for the vacuum instability (see the right panel in Fig. 1). Now, from (5.14) it follows that the corresponding VEV of the field squared is positive at large distances.

In order to find the leading terms in the asymptotic expansions of the VEVs near the boundary by using the general formulas (5.22) and (5.32), we need the function $B(x)$ in the asymptotic expansion (5.18) for the interior spaces under consideration. This function is found in

Appendix A. By using the expression for the function $C(x)$ from (A10), the integral in (5.22) is expressed in terms of the gamma functions and for the VEV of the field squared one gets

$$\langle\varphi^2\rangle_c$$

$$\approx -\frac{(\xi - \xi_D)\Gamma((D-1)/2)}{2^D\pi^{(D+1)/2}(D-2)a}\frac{C_k(x_a) - 1}{(r-a)^{D-2}}\left[D + \frac{1}{C_k(x_a)}\right]. \qquad (6.32)$$

This leading term does not depend on the mass of the field. For a conformally coupled field it vanishes and the next-to-leading order term should be kept. For a minimally coupled field, near the boundary the VEV of the field squared is negative for the interior dS space and positive for the AdS space.

In Fig. 2, for the dS interior geometry, we have plotted the VEV of the field squared in the exterior region, $\alpha^{D-1}\langle\varphi^2\rangle_c$, in $D = 3$ spatial dimensions, as a function of the ratio r/a. The numbers near the curves are the values of a/α. The left and right panels correspond to minimally ($\xi = 0$) and conformally ($\xi = 1/6$) coupled massless scalars. Similar graphs for the AdS interior geometry are presented in Fig. 3.

In a similar way, from (5.32) for the VEVs of the energy density and the azimuthal stress near the boundary we obtain

$$\langle T_0^0\rangle_c \approx \frac{\Gamma((D+1)/2)[C_k(x_a) - 1]}{2^{D-1}\pi^{(D+1)/2}a(r-a)^D}$$

$$\times \left\{(\xi - \xi_D)\left[D(\xi - \xi_D) + \frac{\xi}{C_k(x_a)}\right]\right.$$

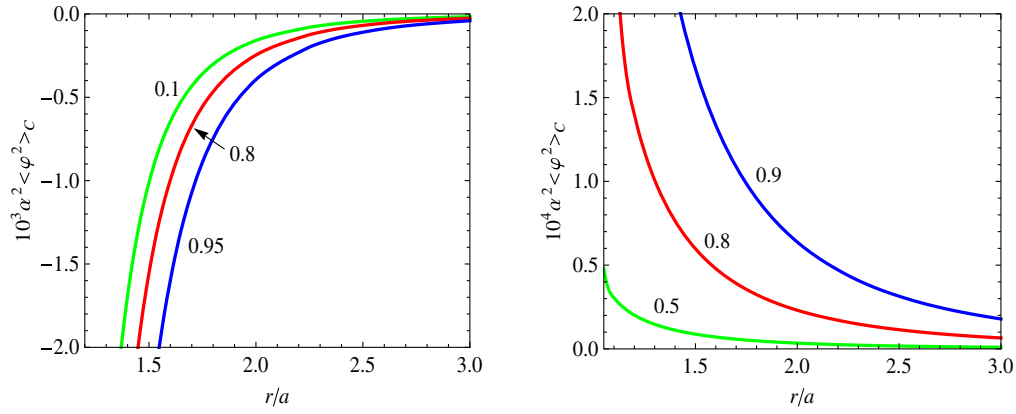$$\left. - \xi_D\frac{(\xi - \xi_{D+2})}{C_k(x_a)}\right\}. \qquad (6.33)$$

FIG. 2 (color online). VEV of the field squared, $\alpha^{D-1}\langle\varphi^2\rangle_c$, for the interior $D = 3$ dS geometry as a function of the rescaled radial coordinate for several values of a/α (with numbers near the curves). The left and right panels correspond to minimally and conformally coupled massless scalar fields.
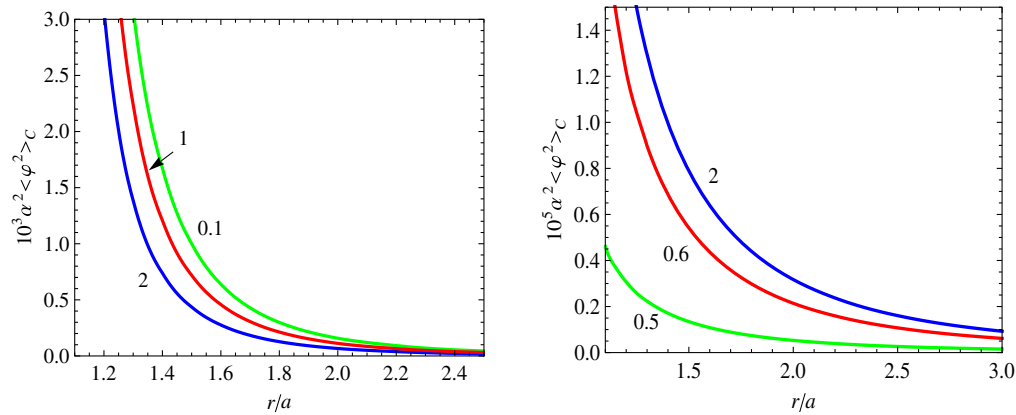

FIG. 3 (color online). The same as Fig. 2 but in the case of the interior AdS space.

and

$$\langle T_2^2\rangle_c \approx \frac{\Gamma((D+1)/2)[C_k(x_a)-1]}{2^{D-1}\pi^{(D+1)/2}a(r-a)^D}$$
$$\times\left\{(\xi-\xi_D)\left[D(\xi-\xi_D)+\frac{\xi-1/4}{C_k(x_a)}\right]+\frac{\xi-\xi_{D+2}}{4DC_k(x_a)}\right\},$$
(6.34)

where $\xi_{D+2} = (D+1)/(4(D+2))$. The leading term in the asymptotic expansion of the radial stress is found by using the relation (5.33). For a minimally coupled field, the energy density, $\langle T_0^0\rangle_c$, and azimuthal stress, $\langle T_2^2\rangle_c$, are negative near the boundary for the dS interior space and are positive for the AdS interior. The expressions (6.33) and (6.34) are further simplified for a conformally coupled field

$$\langle T_2^2\rangle_c \approx -\frac{1}{D-1}\langle T_0^0\rangle$$
$$\approx \frac{\Gamma((D+1)/2)[1/C_k(x_a)-1]}{2^{D+3}\pi^{(D+1)/2}D^2(D+2)a(r-a)^D}.$$
(6.35)

In this case, near the boundary the vacuum energy and the azimuthal pressure ($-\langle T_2^2\rangle_c$) are negative for the interior dS space and are positive for the AdS space.

Figure 4 displays the VEV of the energy density, $\alpha^{D+1}\langle T_0^0\rangle_c$, induced by the interior $D = 3$ dS (left panel) and AdS (right panel) geometries, for a conformally coupled massless scalar field, as a function of the rescaled radial coordinate. The numbers near the curves correspond to the values of the parameter a/α. The corresponding graphs for a massless minimally coupled scalar field show similar behavior.

It is also of interest to consider the dependence of the VEVs on the mass of the field. In Fig. 5 we have plotted the VEV of the energy density in the exterior region as a function of $m\alpha$, for fixed values $a/\alpha = 0.5$, $r/a = 1.5$, in the cases of minimally (left panel) and conformally (right panel) coupled fields in $D = 3$ spatial dimensions. The full and dashed curves correspond to interior dS and AdS spaces. As is seen from the graphs, the VEV is not a monotonic function of the mass.

In the investigation of the VEVs for the case of the interior dS space, we have assumed that $\alpha/a > 1$. For the
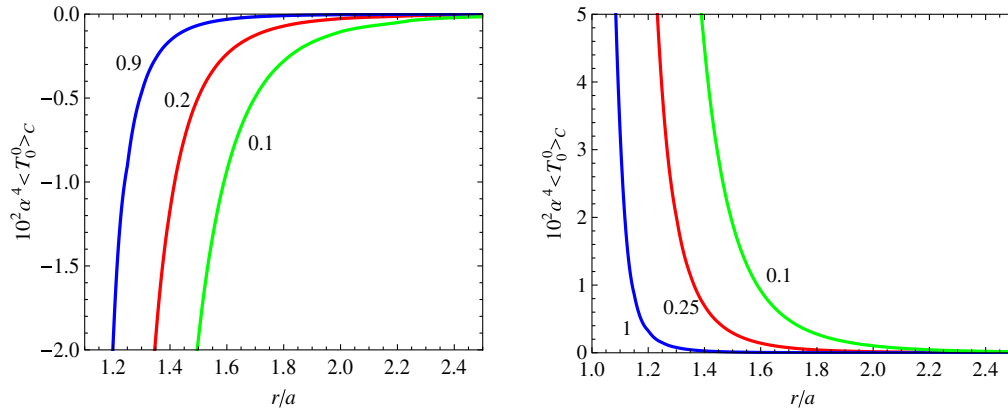
FIG. 4 (color online). VEV of the energy density $\alpha^{D+1}\langle T_0^0\rangle_c$ for a conformally coupled massless field, induced by the interior $D = 3$ dS space (left panel) and AdS (right panel) spaces, versus r/a. The numbers near the curves correspond to the values of the ratio a/α.
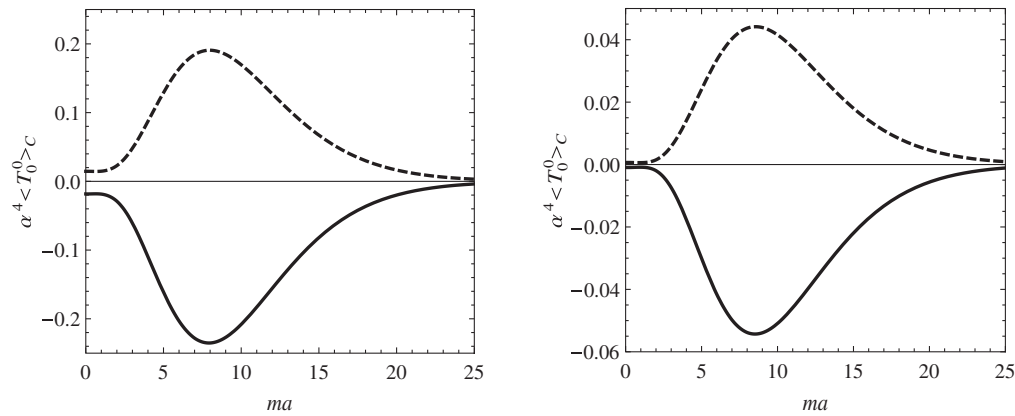

FIG. 5. VEV of the energy density in the exterior region as a function of $m\alpha$ for fixed $a/\alpha = 0.5$ and $r/a = 1.5$. The left and right panels correspond to minimally and conformally coupled scalar fields in $D = 3$ spatial dimensions and the full and dashed curves correspond to dS and AdS interiors.

interior AdS space, the value of this ratio can be arbitrary. In this case, it is of interest to consider the behavior of the VEVs for small values of the AdS curvature radius, $\alpha/a \ll 1$, corresponding to a strong gravitational field in the interior region. In this limit, the argument of the hypergeometric functions in (6.25) is close to 1; $(1 - z_a) \ll 1$. By using the formula 15.3.6 from [21], to the leading order we get

$$F_{\nu_l}(\eta, z_a) \approx (\alpha/a)^{-2\nu/\nu_l}. \qquad (6.36)$$

The coefficient of the function $F(z)$ in (5.6) becomes $(a/\alpha)^{\nu'}$ with the notation $\nu' = \nu + 2\xi D - D/2$. For $\nu' \neq 0$, in the limit under consideration, this coefficient is large and, in the leading order, the VEVs in the exterior region coincide with the corresponding VEVs for a spherical boundary in Minkowski spacetime with the Dirichlet boundary condition. For $\nu' = 0$, the next-to-leading term in the expansion over α/a should be taken into account. Keeping this term, we can see that the VEVs are reduced to

those for a spherical shell with Dirichlet and Neumann boundary conditions in the cases $\nu < 1/2$ and $\nu > 1/2$, respectively. The case $\nu' = 0$ with $\nu = 1/2$ corresponds to a conformally coupled massless scalar field and in this case the VEVs are not reduced to Dirichlet or Neumann results. If, in addition, we assume that $\alpha m \ll 1$, then the condition $\nu' = 0$ is satisfied for the special cases of minimally and conformally coupled fields. We expect that, for small values of the AdS curvature radius, the VEVs in the interior region will be suppressed. This sort of suppression in the boundary-induced local VEVs for the geometry of parallel plates in AdS bulk, described in Poincaré coordinates, has been discussed in [25–27] for scalar and fermionic fields.

We have considered the VEVs in a combined geometry with interior dS or AdS and exterior Minkowski spacetimes. It would be interesting to generalize the corresponding results for the exterior Schwarzschild solution of the Einstein equations. The possibility that the interior geometry of a black hole could be constituted by a dS region has

been discussed in the literature (see [28]–[33] and references therein). However, in the Schwarzshild geometry the equation for the radial part of the scalar mode functions is not exactly solvable and numerical or approximate results only can be provided.

VII. CONCLUSION

In the present paper we have considered the Casimir densities for a scalar field with a general curvature coupling parameter, induced by a spherical boundary separating the spacetime backgrounds with different geometries. The latter are described by spherically symmetric static line elements (2.1) and (2.3) for the interior and exterior regions, respectively. Additionally, the presence of an infinitely thin spherical shell with a surface energy-momentum tensor τ_i^k is assumed. The interior and exterior metric tensors are continuous on the separating boundary and their radial derivatives are related by the Israel matching conditions. The latter lead to the relations (2.9) for the functions in the expressions of the metric tensor components. The matching conditions for a scalar field are obtained from the corresponding field equation: the field is continuous on the separating surface and the jump in the radial derivative is given by the relation (3.3). The jump comes from the nonminimal coupling of the field and is a consequence of the delta function term in the Ricci scalar located on the separating boundary.

For the investigation of the exterior vacuum properties induced by the interior geometry, first we evaluate the positive frequency Wightman function with the help of the direct summation over a complete set of field modes. In Sec. III, for the general cases of interior and exterior geometries, we have constructed a complete set of normalized mode functions obeying the matching conditions. In addition to the modes with a continuous energy spectrum, depending on background geometry, the modes describing the bound states can be present. For these modes, the quantum number λ is purely imaginary and the corresponding eigenvalues for $\eta = |\lambda|$ are solutions of the equation (3.31) with the notation (3.32). The Wightman function in the exterior region is given by the expression (4.2) for the modes with a continuous energy spectrum and by (4.9) for the contribution coming from the bound states. In order to separate from the expression of the Wightman function the part induced by the interior geometry, we use the identity (4.5). Then, by using the asymptotic properties of the radial parts in the mode functions, we rotate the contours of the integration in the complex plane λ. As a result, the Wightman function in the exterior region is presented in a decomposed form (4.11). In this representation, the function $W_0(x, x')$ is the Wightman function in the case of the background described by the line element (2.3) for all values of the radial coordinate r and the contribution $W_c(x, x')$ is induced by the geometry (2.1) in the region $r < a$. Compared with the initial form, the representation

(4.11) of the Wightman function has two important advantages. First of all, in the part induced by the interior geometry the integrand is an exponentially decreasing function at the upper limit of the integration, instead of highly oscillatory behavior in the initial representation. And, second, for points outside the boundary, the divergences arising in the coincidence limit of the arguments are contained in the part $W_0(x, x')$, whereas the part induced by the interior geometry is finite in the coincidence limit. With this property, the renormalization of the VEVs for the field squared and the energy-momentum tensor is reduced to the renormalization for the background (2.3) for all values of r. Hence, the contributions to the VEVs coming from the interior geometry are directly obtained from the corresponding part of the Wightman function without any additional subtractions.

For a given Wightman function, the VEVs of the field squared and the energy-momentum tensor are evaluated by formulas (4.12). They are decomposed as (4.13), where the second terms in the right-hand sides are induced by the geometry (2.1) in the region $r < a$. These terms are obtained from the corresponding part in the Wightman function without additional renormalization. For example, the VEV of the field squared is given by (4.15).

A special case, with the Minkowski spacetime as an exterior geometry, is discussed in Sec. V. In this case the expression for the Wightman function in the exterior region is reduced to (5.5). The latter differs from the corresponding expression for a spherical boundary with the Robin boundary condition by the replacement (5.10) of the Robin coefficient. In the geometry under consideration, the "effective" Robin coefficient depends on the quantum numbers specifying the scalar field modes and this leads to important modifications in the behavior of the VEVs near the boundary. For the exterior Minkowskian geometry, the VEVs of the field squared and the energy-momentum tensor are given by the expressions (5.11) and (5.23). For a massive field, at distances from the boundary larger than the Compton wavelength, the VEVs are exponentially suppressed. For a massless field, the decay of the VEVs at large distances is a power law: it goes like r^{3-2D} for the field squared and like r^{1-2D} for the energy-momentum tensor. The exponents in the power-law decay are different in the special cases $\beta_0 = \pm(D/2 - 1)$ with β_0 defined by (5.15). The VEVs diverge on the boundary separating the interior and exterior geometries. The leading terms in the asymptotic expansions over the distance from the boundary are given by (5.22) for the field squared and by (5.32) for the energy density and the azimuthal stress. For the radial stress near the boundary, one has (5.33). The function $C(x)$ in the expressions for the leading terms is determined from the uniform asymptotic expansion of the interior radial mode function for large values of the orbital momentum and it depends on the specific interior geometry. The VEV of the field squared diverges on the boundary

as $(r/a - 1)^{2-D}$ and the VEVs of the energy density and the azimuthal stress diverge as $(r/a - 1)^{-D}$. In the case of a spherical boundary in Minkowski spacetime with Dirichlet and Neumann (or, in general, Robin) boundary conditions, the surface divergences are stronger.

As an application of general results, in Sec. VI we have considered dS and AdS spaces as examples of the interior geometry. First, we have transformed the corresponding line elements to the form (6.7), which is continuously matched with the exterior Minkowskian geometry. The components of the corresponding surface energy-momentum tensor are given by (6.11). The radial parts of the interior mode functions are expressed in terms of the hypergeometric function [(6.14) and (6.16) for regular and irregular modes, respectively]. The VEVs of the field squared and the energy-momentum tensor in the exterior Minkowskian region are determined by the formulas (5.11) and (5.23), where in the expressions for $\tilde{I}_{\nu_l}(a\eta)$ and $\tilde{K}_{\nu_l}(a\eta)$, defined by (5.6), the functions (6.18) and (6.24) should be substituted. In the case of the interior AdS geometry, there are no bound states. For the dS interior, the same holds for a minimally coupled field. In the case of the dS interior geometry and for nonminimally coupled fields, bound states are absent if the radius of the separating boundary is not too close to the dS horizon radius. When the boundary becomes closer to the horizon, bound states appear. With the further increasing of the boundary radius, the energy of the bound state decreases, and for some critical value it becomes zero. The further increase leads to imaginary values of the energy thus signaling the exterior Minkowski vacuum instability.

In the cases of dS and AdS interior spaces, we have specified the general formulas for the asymptotics of the VEVs. The parameter β_0, determining the large distance behavior of the VEVs for massless fields, is given by the expression (6.27). For a minimally coupled field, one has $\beta_0 = D/2 - 1$, and the leading terms in the asymptotic expansion of the VEVs at large distances vanish. The leading terms in the expansions near the boundary are given by the expressions (6.32), (6.33), and (6.34). For a conformally coupled field, the leading term in the VEV of the field squared vanishes. In this case, near the boundary the vacuum energy and the azimuthal pressure are negative for the interior dS space and are positive for the AdS space. For a minimally coupled field and near the boundary, the VEVs of the field squared, energy density, and azimuthal stress are negative for the interior dS space and positive for the AdS space. In the latter case and for small values of the AdS curvature radius (the strong gravitational field in the interior region), $\alpha \ll a, m^{-1}$; for the curvature coupling parameter $\xi \neq 0, \xi_D$, the VEVs in the exterior region, to the leading order, coincide with the corresponding VEVs for a spherical boundary in Minkowski spacetime with the Dirichlet boundary condition. For a minimally coupled field, the VEVs are

reduced to those for a spherical shell with the Neumann boundary condition. In the special case of the conformal coupling, the VEVs are not reduced to Dirichlet or Neumann results.

The results given above for gravitational backgrounds may have applications in effective field theoretical models of some condensed matter systems formulated on curved backgrounds (see, for example, [7,34]). Important examples of this sort are graphene-made structures. The long-wavelength description of the graphene excitations can be formulated in terms of the effective field theory in $(2 + 1)$-dimensional spacetime. In the geometry of a single-walled carbon nanotube, which is generated by rolling up a graphene sheet to form a cylinder, the background space is flat and has the topology $R^1 \times S^1$. For nanotubes with open ends, the Casimir densities induced by the nontrivial topology and by the edges have been discussed in [35–37]. However, the end of the nanotube can be closed with a hemispherical cap. In this case the geometry for the corresponding effective field theory is of the type discussed above with the interior constant curvature space.

ACKNOWLEDGMENTS

APPENDIX: ASYMPTOTIC OF THE HYPERGEOMETRIC FUNCTION

As it has been shown in Sec. V, the leading terms of the asymptotic expansions for the VEVs near the spherical boundary, separating the regions with different geometries, are expressed in terms of the function $C(x)$ given by (5.20). In this expression, $B(x)$ is defined by the asymptotic expansion of the function $y_l(a, \nu_l \eta)$ for the large ν_l [see (5.18)]. In order to find the function $B(x)$ for the special cases of the interior geometry corresponding to dS and AdS spaces, in accordance with (6.21), we need the asymptotic of the function $F_{\nu_l}(\nu_l \lambda, z_a)$ for large values of ν_l. The leading term is obtained from the general consideration given above, and for the determination of the function $B(x)$ we need the next-to-leading term. In the limit under consideration, all the parameters of the hypergeometric functions in (6.25) are large. The corresponding asymptotics have been recently investigated in [38,39]. By using the expansion (2.8) from [39], for large $|\mu|$ the following result can be obtained:

$$\frac{F(a + \varepsilon_1\mu, b + \varepsilon_2\mu; c + \mu - 1; z)}{F(a + \varepsilon_1\mu, b + \varepsilon_2\mu; c + \mu; z)}$$
$$\sim \frac{1 - \varepsilon_1}{1 - t_s}\left[1 + \frac{h(t_s)}{\mu} + \cdots\right], \tag{A1}$$

where $0 < \varepsilon_1 \leq \varepsilon_2 < 1$ and (in notations of [39])

$$t_s = \frac{\Delta - \sqrt{\Delta^2 - 4\varepsilon_1(1 - \varepsilon_2)z}}{2(1 - \varepsilon_2)z}, \qquad \Delta = 1 + (\varepsilon_1 - \varepsilon_2)z.$$
$$\text{(A2)}$$

In (A1), we have defined the function

$$h(t) = \frac{(c - 1)\varepsilon_1 - a}{1 - \varepsilon_1} - \frac{t}{h_1(t)} \left\{ [(c - 3)\varepsilon_2 - b]t + b\varepsilon_1 \right.$$
$$- \varepsilon_2(a - 1) + \frac{1}{h_1(t)}[(\varepsilon_2^2 - 1)(t - 3\varepsilon_1)t^2$$
$$\left. + 3\varepsilon_1(\varepsilon_2^2 - \varepsilon_1)t + \varepsilon_1(\varepsilon_1^2 - \varepsilon_2^2)] \right\}, \qquad \text{(A3)}$$

with

$$h_1(t) = \varepsilon_1(\varepsilon_2 - \varepsilon_1) + t(2\varepsilon_1 - t)(1 - \varepsilon_2). \qquad \text{(A4)}$$

In order to apply (A1) to the function $F_{\nu_l}(\nu_l\eta, z_a)$ [defined by (6.25)] with $\mu = \nu_l$, we assume for the moment that $k = -1$. In this case the parameters ε_j corresponding to (A1) are real. We are interested in the term of the order $1/\nu_l$, and, to this order, the mass term in (6.26) does not contribute. Assuming that the parameters are in the range required for the validity of (A1), we take in this expansion

$$a = b = \frac{1}{2}(1 + \nu), \qquad c = 1,$$
$$\varepsilon_1 = \frac{1}{2}(1 - \gamma), \qquad \varepsilon_2 = \frac{1}{2}(1 + \gamma), \qquad \text{(A5)}$$

with

$$\gamma = \eta\sqrt{\alpha^2 - a^2}. \qquad \text{(A6)}$$

For these values of the parameters, one has

$$2\frac{1 - \varepsilon_1}{1 - t_s} = 1 + \sqrt{1 - a^2/\alpha^2}\sqrt{1 + a^2\eta^2}. \qquad \text{(A7)}$$

In the leading order this gives

$$2F_{\nu_l}(\nu_l\eta, z_a) \sim 1 + \sqrt{1 - a^2/\alpha^2}\sqrt{1 + a^2\eta^2}. \qquad \text{(A8)}$$

Substituting into (6.24), we obtain the leading term for the expansion of the function $y_l(a, \nu_l\lambda)$, which agrees with the result (5.18) obtained directly from the differential equation for $y_l(a, \eta)$.

Evaluating the function $h(t)$ for special values of the parameters (A5), (A6) and substituting the corresponding expansion (A1) into the expression (6.24) with $\eta \to \nu_l\eta$, after long calculations we find the expansion (5.18) with the function

$$B(u) = \frac{(1 + u^2)^{-1} - (D - 1)(1 - a^2/\alpha^2)}{2\sqrt{1 - a^2/\alpha^2}\sqrt{1 + u^2}}, \qquad \text{(A9)}$$

and $u = \eta a$. Although we have obtained the formula (A9) in the range of parameters assumed for the validity of (A1), the corresponding formula for other values of ηa is obtained by a simple analytic continuation. Moreover, the result can also be generalized for the case of AdS space by the replacement $\alpha \to i\alpha$. Having the expression for the function $B(u)$, the function $C(u)$ is found from (5.20):

$$C(u) = 2\frac{C_k(x_a) - 1}{\sqrt{1 + u^2}} \left[D(\xi - \xi_D) + \frac{\xi}{C_k(x_a)} - \frac{(1 + u^2)^{-1}}{4C_k(x_a)} \right]. \qquad \text{(A10)}$$

With this function, the integrals in the expressions (5.22) and (5.32) of the leading terms in the VEVs of the field squared and the energy-momentum tensor are expressed in terms of the gamma function.

---

[1] H. B. G. Casimir, Proc. K. Ned. Akad. Wet. **51**, 793 (1948).

[2] V. M. Mostepanenko and N. N. Trunov, *The Casimir Effect and its Applications* (Clarendon, Oxford, 1997).

[3] E. Elizalde, S. D. Odintsov, A. Romeo, A. A. Bytsenko, and S. Zerbini, *Zeta Regularization Techniques with Applications* (World Scientific, Singapore, 1994).

[4] K. A. Milton, *The Casimir Effect: Physical Manifestation of Zero-Point Energy* (World Scientific, Singapore, 2002).

[5] M. Bordag, G. L. Klimchitskaya, U. Mohideen, and V. M. Mostepanenko, *Advances in the Casimir Effect* (Oxford University Press, Oxford, 2009).

[6] *Casimir Physics*, edited by D. Dalvit, P. Milonni, D. Roberts, and F. da Rosa, Lecture Notes in Physics Vol. 834 (Springer-Verlag, Berlin, 2011).

[7] F. R. Klinkhamer and G. E. Volovik, Phys. Lett. A **347**, 8 (2005).

[8] E. R. Bezerra de Mello, V. B. Bezerra, A. A. Saharian, and A. S. Tarloyan, Phys. Rev. D **74**, 025017 (2006).

[9] W. A. Hiscock, Phys. Rev. D **31**, 3288 (1985).

[10] J. R. Gott, Astrophys. J. **288**, 422 (1985).

[11] B. Allen and A. C. Ottewill, Phys. Rev. D **42**, 2669 (1990).

[12] E. R. Bezerra de Mello and A. A. Saharian, J. High Energy Phys. 10 (2006) 049.

[13] E. R. Bezerra de Mello and A. A. Saharian, Phys. Rev. D **75,** 065019 (2007).

[14] K. Milton and A. A. Saharian, Phys. Rev. D **85,** 064005 (2012).

[15] A. A. Saharian and A. L. Mkhitaryan, J. High Energy Phys. 08 (2007) 063.

[16] A. A. Saharian and A. L. Mkhitaryan, J. Phys. A **41,** 164062 (2008).

[17] N. D. Birrell and P. C. W. Davies, *Quantum Fields in Curved Space* (Cambridge University Press, Cambridge, England, 1982).

[18] A. Erdélyi *et al.*, *Higher Transcendental Functions* (McGraw-Hill, New York, 1953), Vol. 2.

[19] A. A. Saharian, Phys. Rev. D **69,** 085005 (2004).

[20] A. A. Saharian, Phys. Rev. D **63,** 125007 (2001).

[21] *Handbook of Mathematical Functions*, edited by M. Abramowitz and I. A. Stegun (Dover, New York, 1972).

[22] D. Polarski, Classical Quantum Gravity **6,** 893 (1989).

[23] P. Breitenlohner and D. Z. Freedman, Ann. Phys. (N.Y.) **144,** 249 (1982).

[24] L. Mezincescu and P. K. Townsend, Ann. Phys. (N.Y.) **160,** 406 (1985).

[25] A. A. Saharian, Nucl. Phys. **B712,** 196 (2005).

[26] A. A. Saharian, Phys. Rev. D **73,** 064019 (2006).

[27] E. Elizalde, S. D. Odintsov, and A. A. Saharian, Phys. Rev. D **87,** 084003 (2013).

[28] S. K. Blau, E. I. Guendelman, and A. H. Guth, Phys. Rev. D **35,** 1747 (1987).

[29] W. Shen and S. Zhu, Phys. Lett. **126A,** 229 (1988).

[30] V. P. Frolov, M. A. Markov, and V. F. Mukhanov, Phys. Rev. D **41,** 383 (1990).

[31] E. Farhi, A. H. Guth, and J. Guven, Nucl. Phys. **B339,** 417 (1990).

[32] P. O. Mazur and E. Mottola, Proc. Natl. Acad. Sci. U.S.A. **101,** 9545 (2004).

[33] I. Dymnikova and E. Galaktionov, Classical Quantum Gravity **22,** 2331 (2005).

[34] G. E. Volovik, *The Universe in a Helium Droplet* (Clarendon, Oxford, 2003).

[35] S. Bellucci1 and A. A. Saharian, Phys. Rev. D **80,** 105003 (2009).

[36] E. Elizalde, S. D. Odintsov, and A. A. Saharian, Phys. Rev. D **83,** 105023 (2011).

[37] S. Bellucci1 and A. A. Saharian, Phys. Rev. D **87,** 025005 (2013).

[38] R. B. Paris, J. Classical Anal. **2,** 183 (2013).

[39] R. B. Paris, J. Classical Anal. **3,** 1 (2013).